COMPOSITION OF THE ISOTROPIC γ RAY BACKGROUND AND DARK MATTER CONSTRAINTS

Di Mauro Mattia

INFN Istituto Nazionale di Fisica Nucleare

SIGIL · VNIVERS · AVGVSTAE · TAVRINORVM

HIGH-ENERGY MESSENGERS: CONNECTING THE NON-TERMAL EXTRAGALACTIC BACKGROUND 2014
CHICAGO JUNE 9-11, 2014

Fermi-LAT all sky maps with 5.4 years of data

ISOTROPIC γ RAY BACKGROUND (IGRB)

Abdo et al. 2010 PRL.104j1101A

- The Fermi Large Area Telescope provides a view of the entire gamma-ray sky from 30 MeV to hundreds GeV.

- Galactic diffuse emission produced via:

  -decay of π^0 produced in protons/interstellar gas collisions
  -Bremsstrahlung of relativistic electrons in gas
  -Inverse-Compton of relativistic electrons with ISRF.

- 1451 resolved sources in the first catalogue.

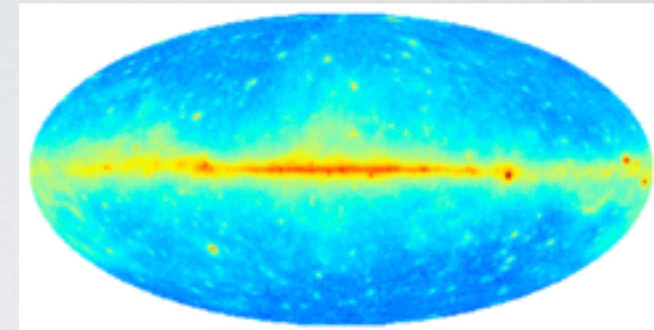

–

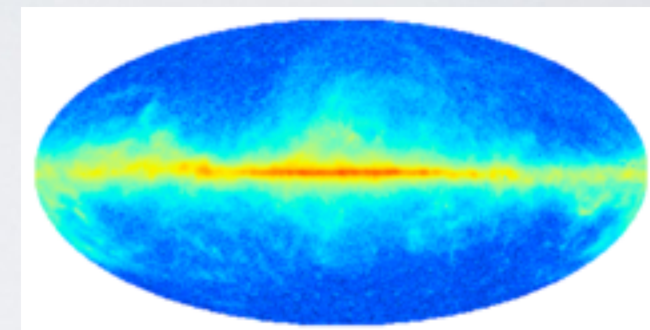

–

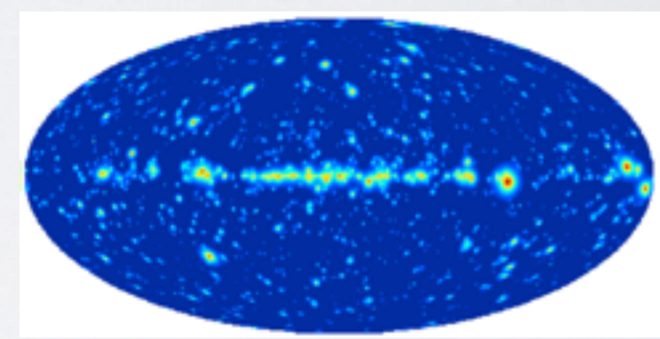

–

Solar Emission

–

CR Background

=

The Fermi-LAT has measured the extragalactic γ-ray background (IGRB) with a very good accuracy

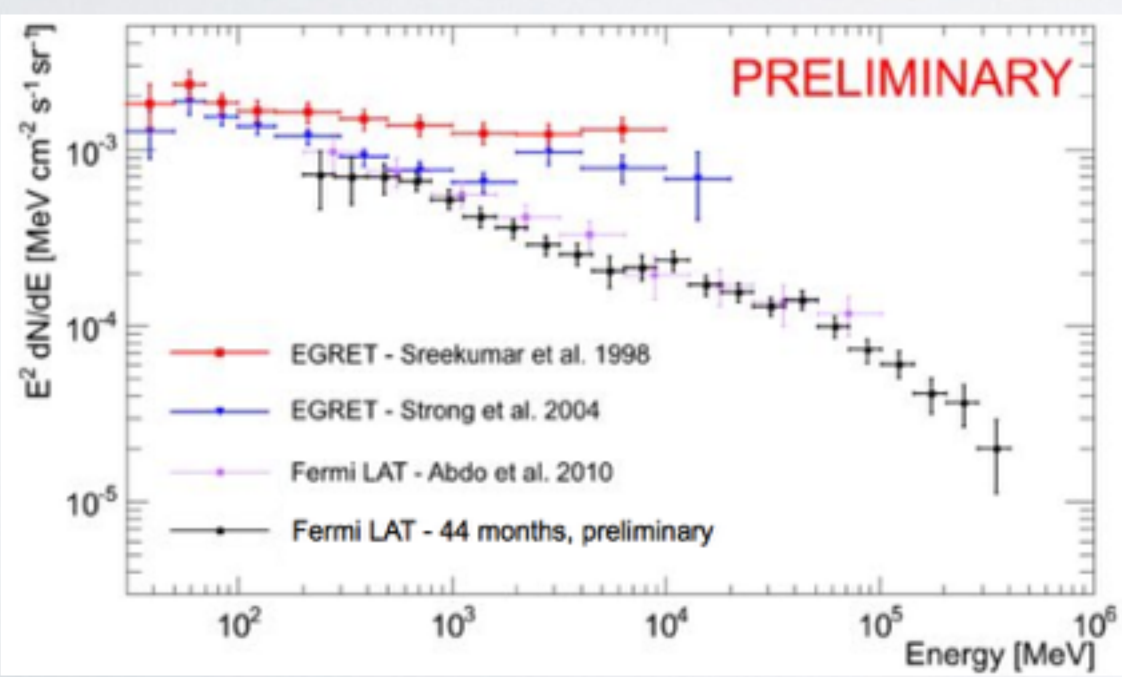

http://galprop.stanford.edu/download/talks/13.Fermi_symposium_Ackermann.pdf

THE ORIGIN OF THE IGRB

Blazars (Bl Lac and FSRQ): 782 detected by Fermi-LAT in the 2FGL. 20%-40% IGRB.

Abdo et al. 2010 ApJ 720 435, Ajello et al. 2012 ApJ 751 108, M. Ajello et al. 2014 ApJ 780 73.

Radio galaxies: 20 detected by Fermi-LAT in the 1FGL and 2 FGL. 20-30% IGRB.

Inoue 2011ApJ 733 66I, Di Mauro et al. 2013 arXiv:1304.0908.

A
G
N

Pulsars: 83 detected by Fermi-LAT. Small contributions expected. few% IGRB. Siegal-Gaskins et al. 2010, Calore et al. 2012 Phys.Rev. D85 (2012) 023004

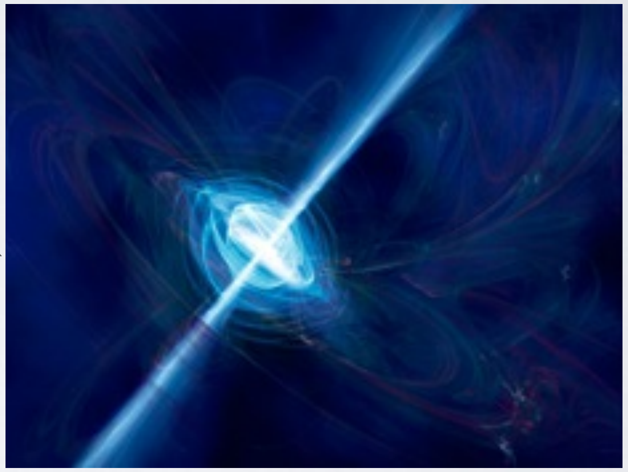

Star-forming galaxies. 4%-23% of IGRB. Ackermann et al. 2012ApJ 755 164A

Dark matter: potential non negligible flux dependent on nature of DM, cross-section and DM distribution.

Other possible sources of γ-rays are:

- **Intergalactic shocks** (Loeb & Waxman 2000, Gabici & Blasi 2003).
- **Interactions of UHE cosmic rays with the EBL** (Kalashev et al. 2009)
- **Extremely large Galactic electron halo** (Keshet et al. 2004)
- **CR interaction in small solar system bodys** (Moskalenko & Porter 2009)

UNRESOLVED EMISSION FROM GALACTIC PULSARS

Diffuse γ-ray emission from misaligned active galactic nuclei.
M. Di Mauro, F. Calore, F. Donato.
In preparation.

PULSARS

Pulsars are rapidly spinning neutron stars

Pulsars divided into young Pulsars (P>0.015 s) and Millisecond Pulsars (MSPs) .

ATNF catalog: about 2000 sources (132 MSPs)

Fermi-LAT second Pulsars catalog (2FPC) with 117 source (40 MSPs and 77 young objects).

From the ATNF catalog we considered the P, B, r and z.

Using dP/dt and P we can derive the spin down luminosity.

The spin down luminosity dE/dt is converted in ɣ-ray luminosity.

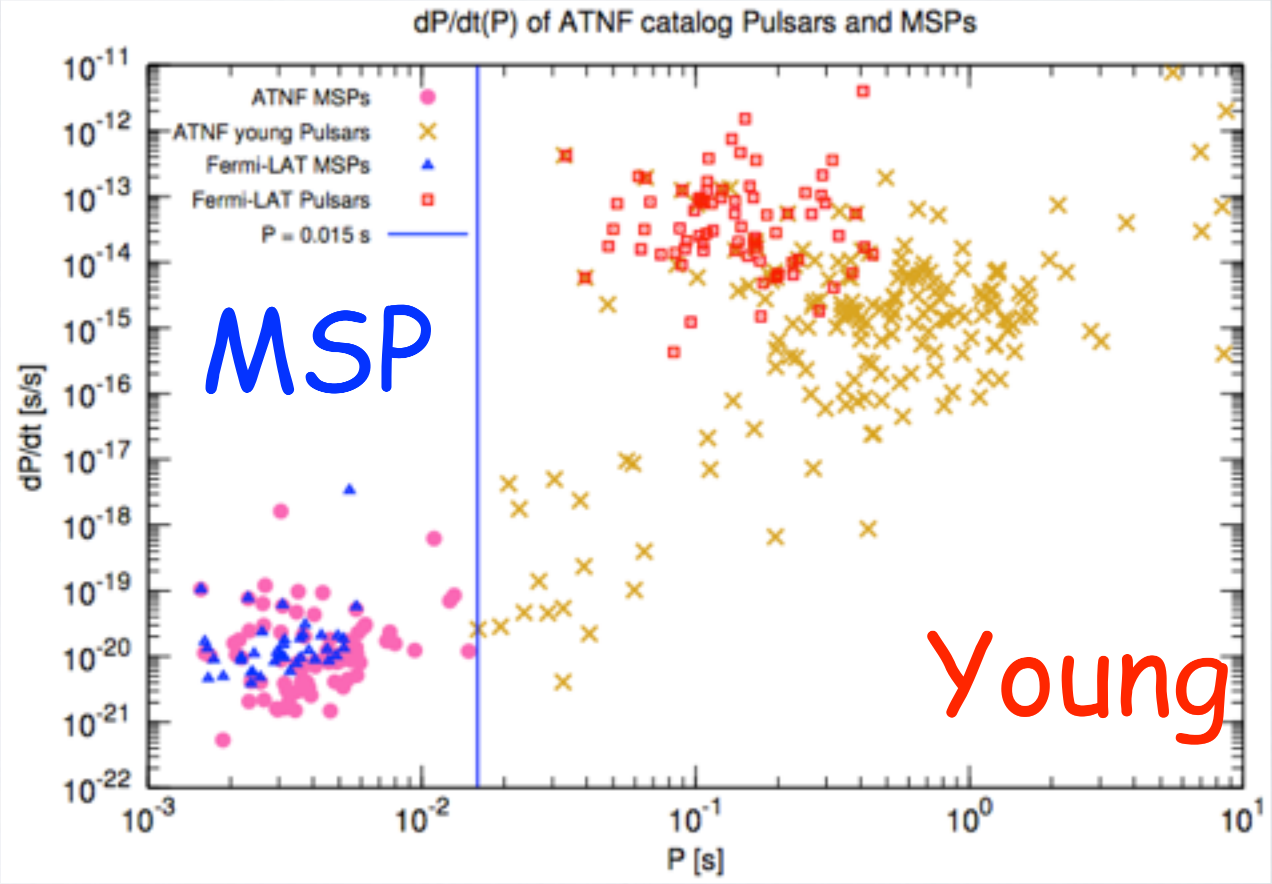

$$\dot{P} = 9.8 \cdot 10^{-26} \left(\frac{B}{\mathrm{G}}\right)^2 \left(\frac{P}{\mathrm{s}}\right)^{-1}$$

$$\dot{E} = 4\pi^2 I \frac{\dot{P}}{P^3}$$

$$L_\gamma = \eta \dot{E}^\alpha$$

Manchester et al. 2005 AJ, 129, 1993

Abdo et al. 2013, apjs, 208, 17

PRELIMINARY

MSP DISTRIBUTIONS

Fro ... alog ...

... istri ...

... 0 kp ...

... plar ...

... c.

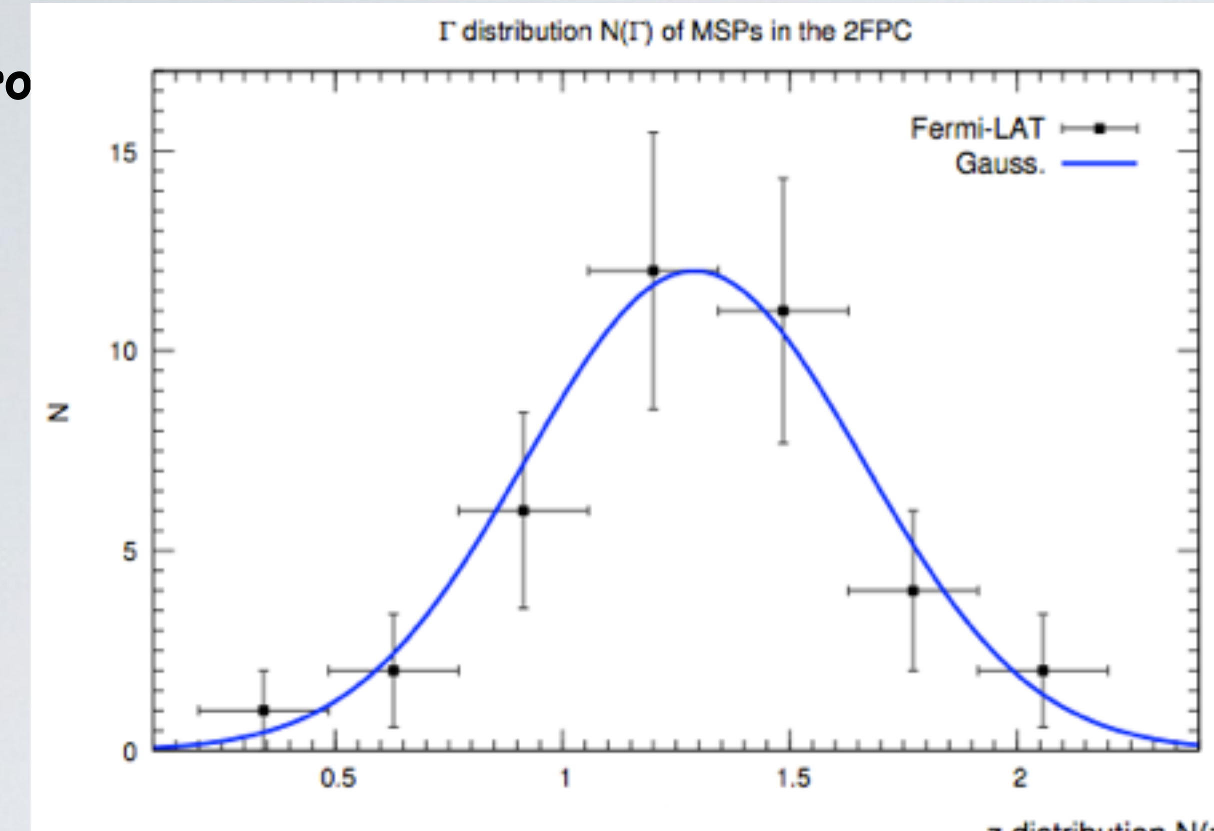

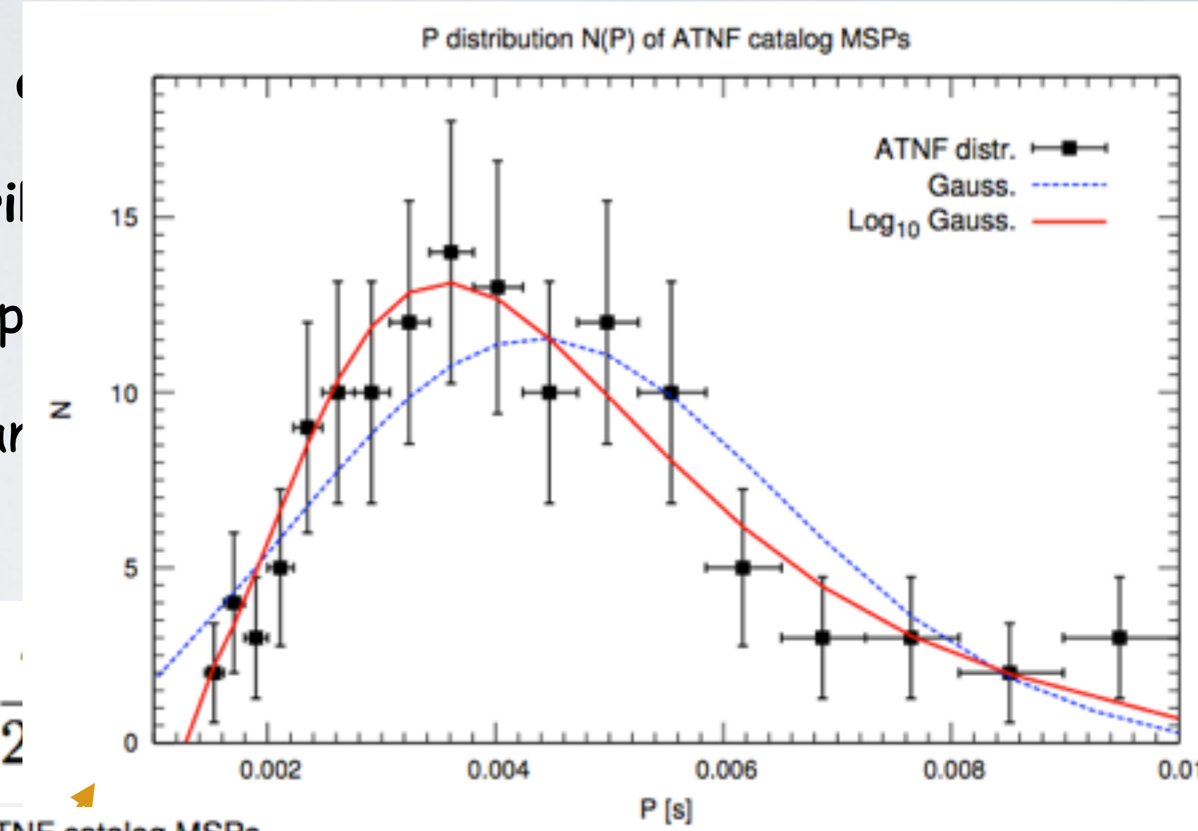

P and I ... rum distribution

- Su ...

  de ...

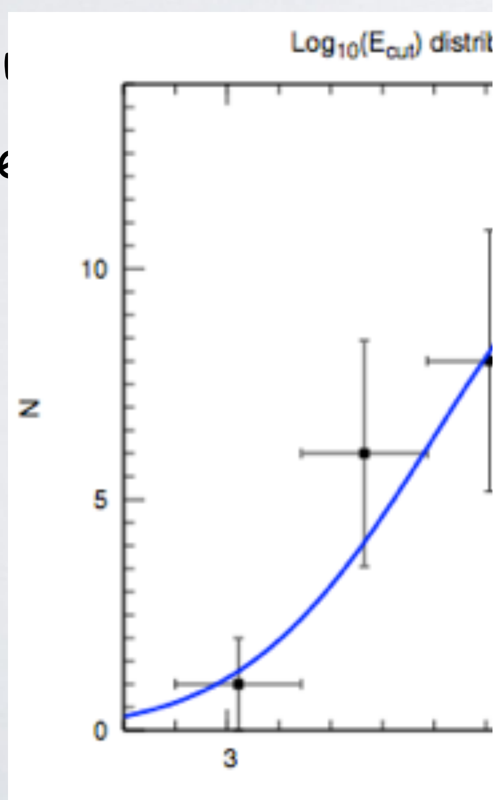

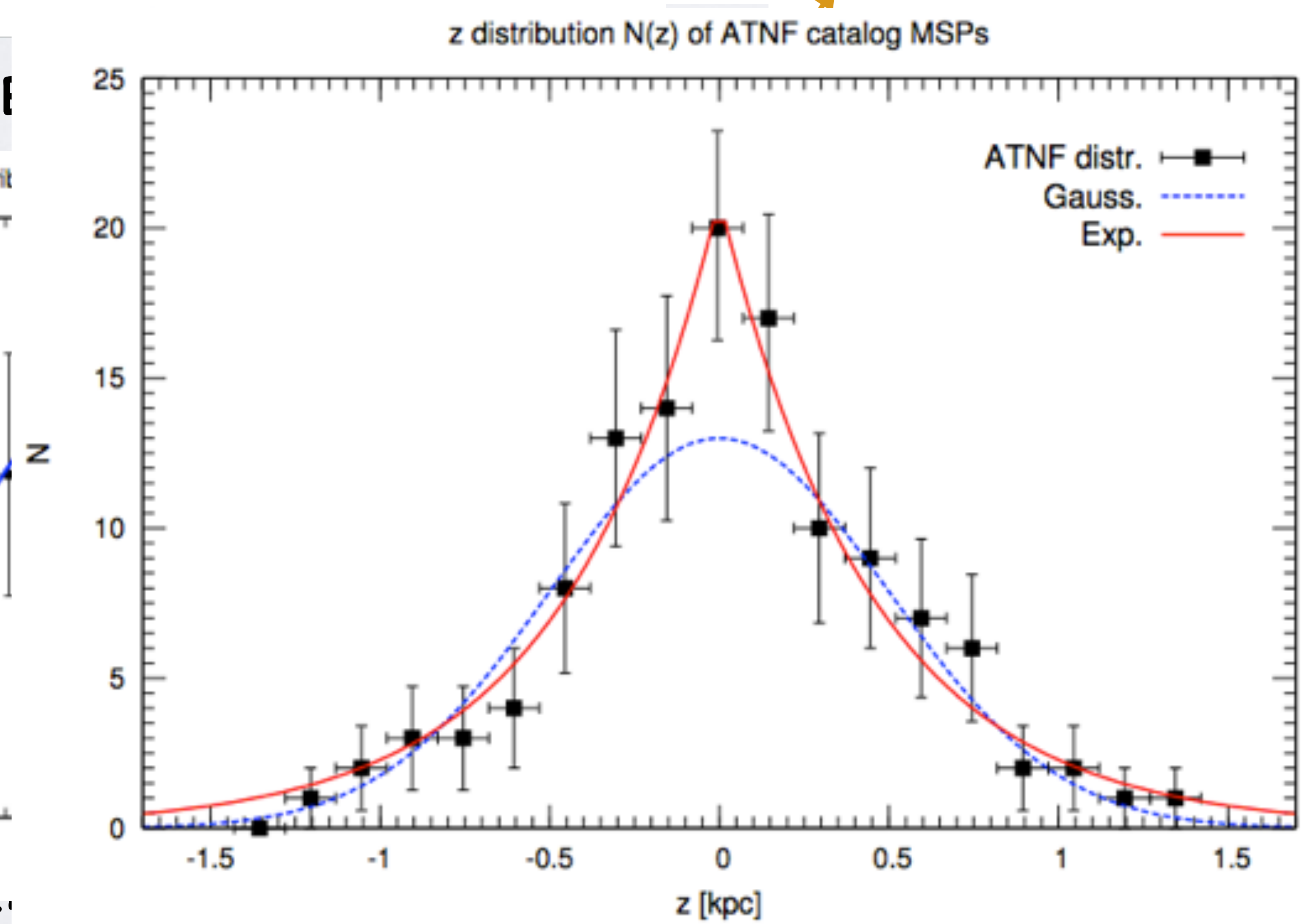

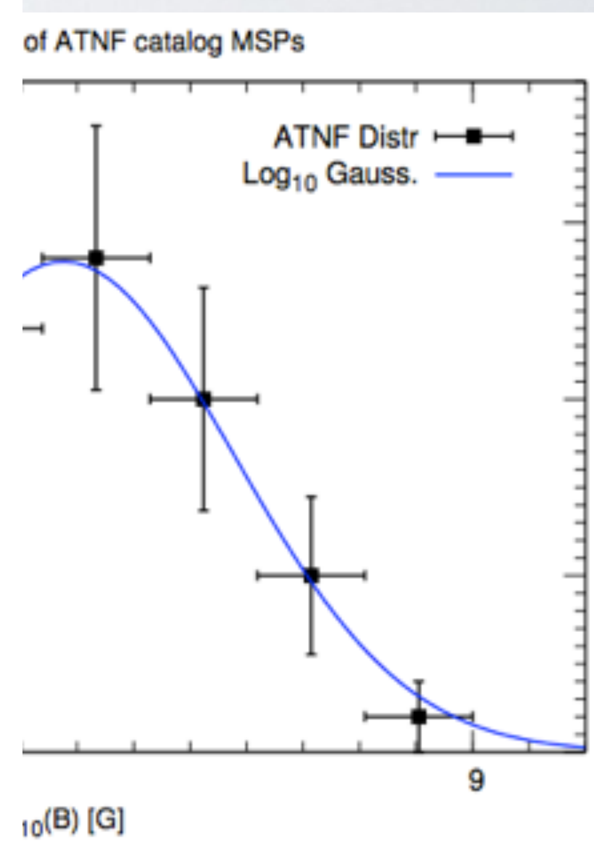

<Log10B>=8. ...

MONTE CARLO METHOD

1

B and P extracted from Log_{10} gaussian distribution. → $\dot{P} = 9.8 \cdot 10^{-26} \left(\frac{B}{\mathrm{G}}\right)^2 \left(\frac{P}{\mathrm{s}}\right)^{-1}$

dE/dt derived from dP/dt and P. $\dot{E} = 4\pi^2 I \frac{\dot{P}}{P^3}$

$L_\gamma = \eta \dot{E}^\alpha$ → L_γ in the range 0.1MeV-100GeV found from L_γ(dE/dt)

2

Radial distance r and the height from the galactic plane z extracted. → $S_\gamma = L_\gamma / (4\pi d^2)$

3

S_γ for the source compared with b-dependent energy flux sensitivity $S_t(b)$

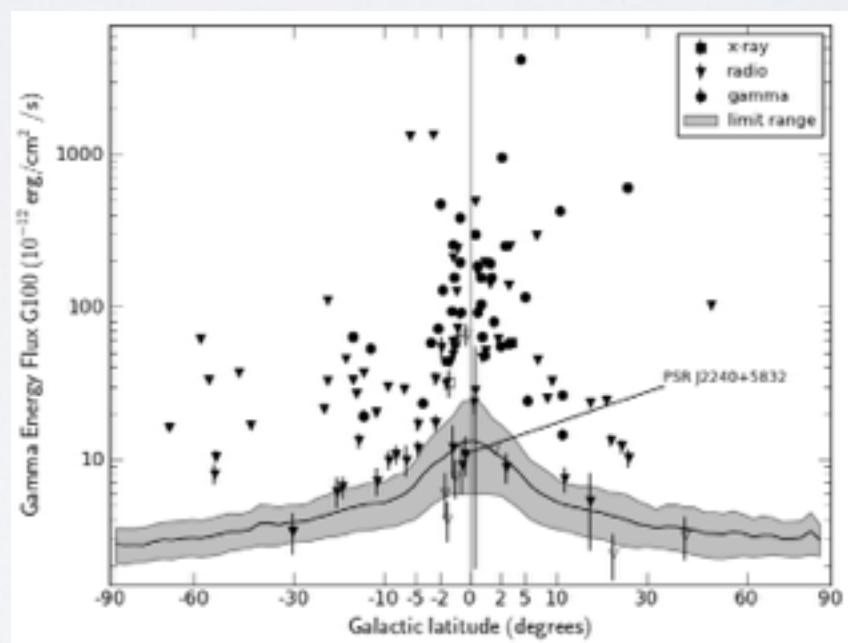

to classify the source as detectable (undetectable) if $S_\gamma > S_t(b)$ ($S_\gamma < S_t(b)$)

4

Γ and E_{cut} extracted for each source.

$S_\gamma \equiv \int_{E_1}^{E_2} \frac{dN}{dE} E\, dE$ and $F_\gamma \equiv \int_{E_1}^{E_2} \frac{dN}{dE} dE$ → $\left(\frac{dN}{dE}(E)\right)_{\mathrm{MSP}} = \frac{1}{\Delta\Omega} \sum_{|b| \geq b_{\min}} \frac{dN}{dE}(E)$

Lγ(dE/dt)

- Effective way to model the MSPs γ-ray emission.

$$L_\gamma = \eta \dot{E}^\alpha$$

- η is the conversion efficiency of spin-down luminosity into γ-ray luminosity.
- Scatter of the data points = impossible to find statistically the relation Lγ(dE/dt).
- We derive 95% C.L. upper limits (ULs) on the γ-ray flux of a sample of 19 sources non-detected by the Fermi-LAT.
- Those sources have been selected in the ATNF catalog as the ones (with b>10°) expected to be the most powerful γ-ray emitters if standard values of α = 1 and η = 0.1 are assumed.

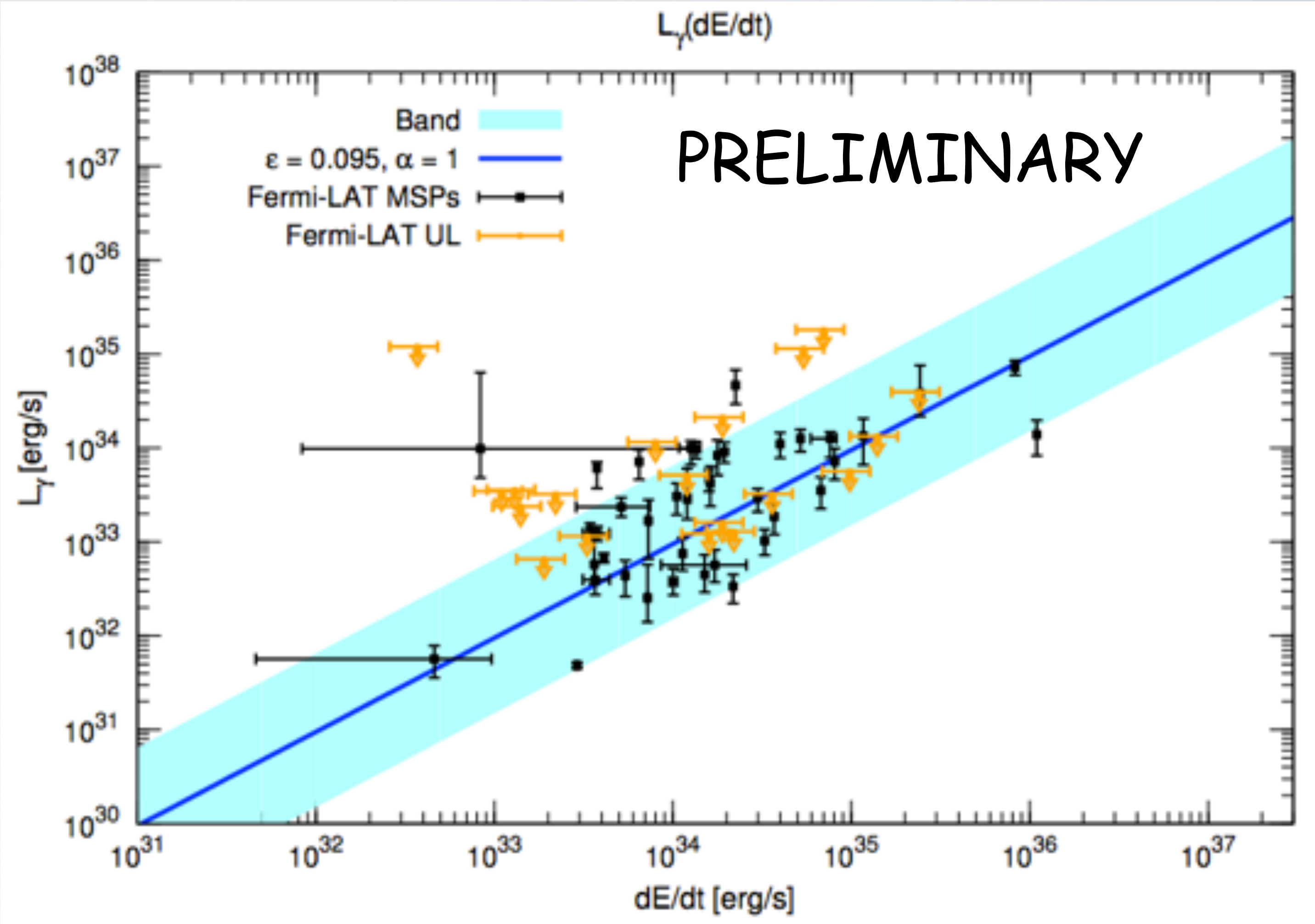

Benchmark relation: α = 1 and η = 0.095 and an uncertainty band with α = 1 and η = {0.015, 0.65}.

MSP DIFFUSE EMISSION AT HIGH LATITUDE

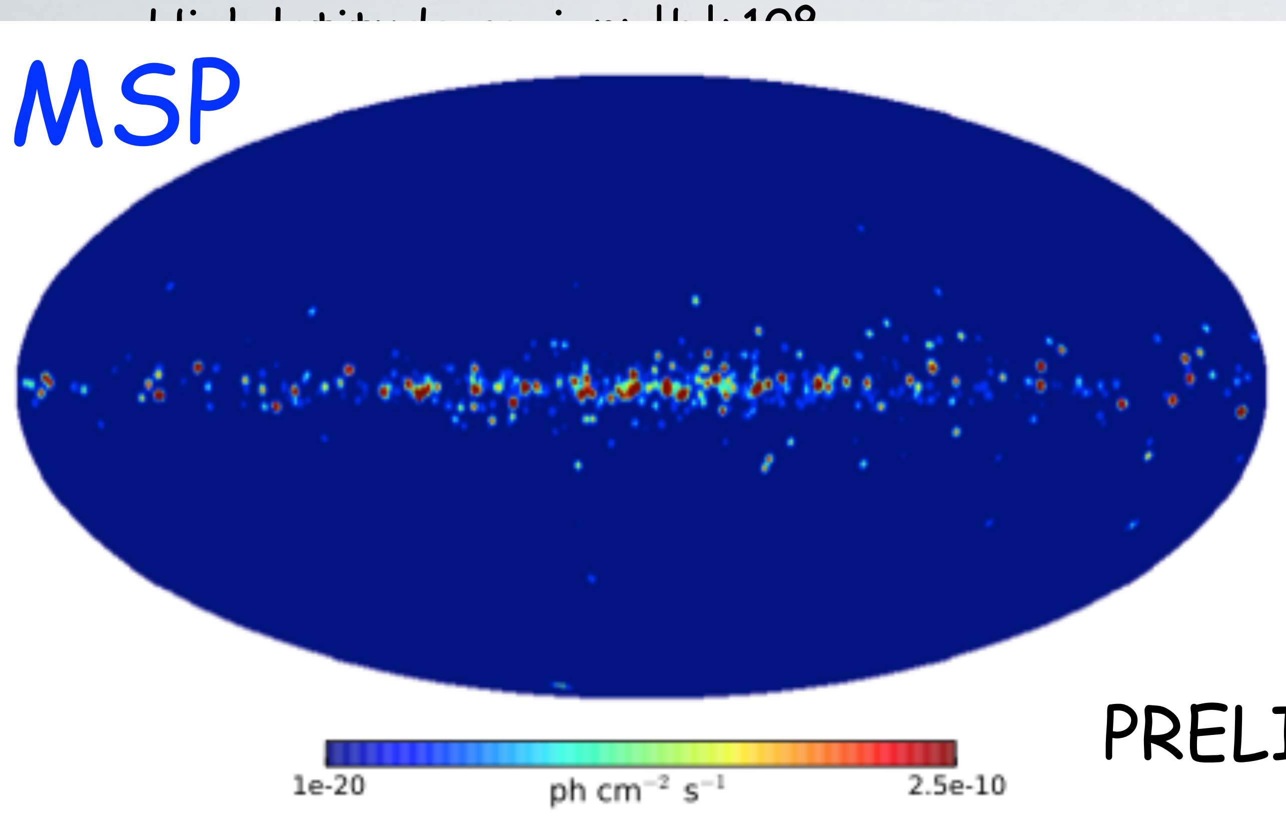

PRELIMINARY

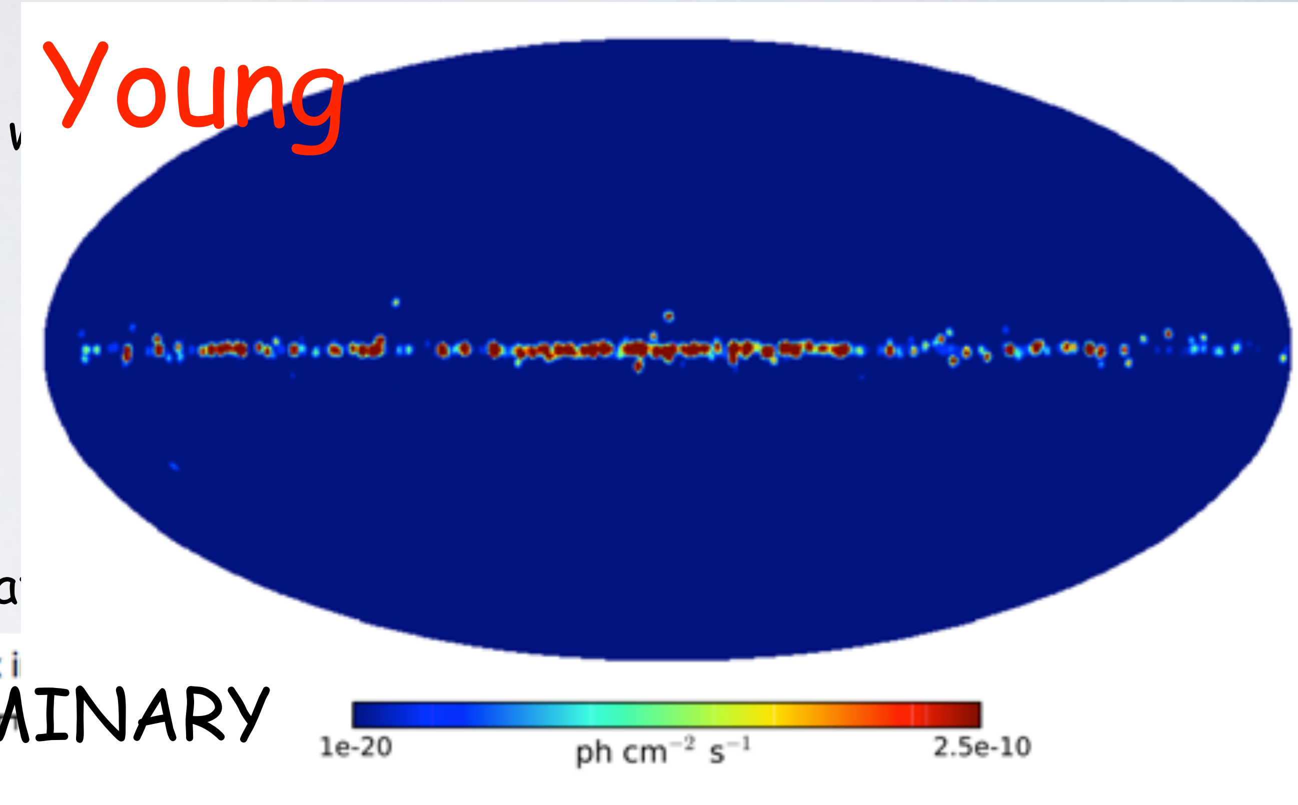

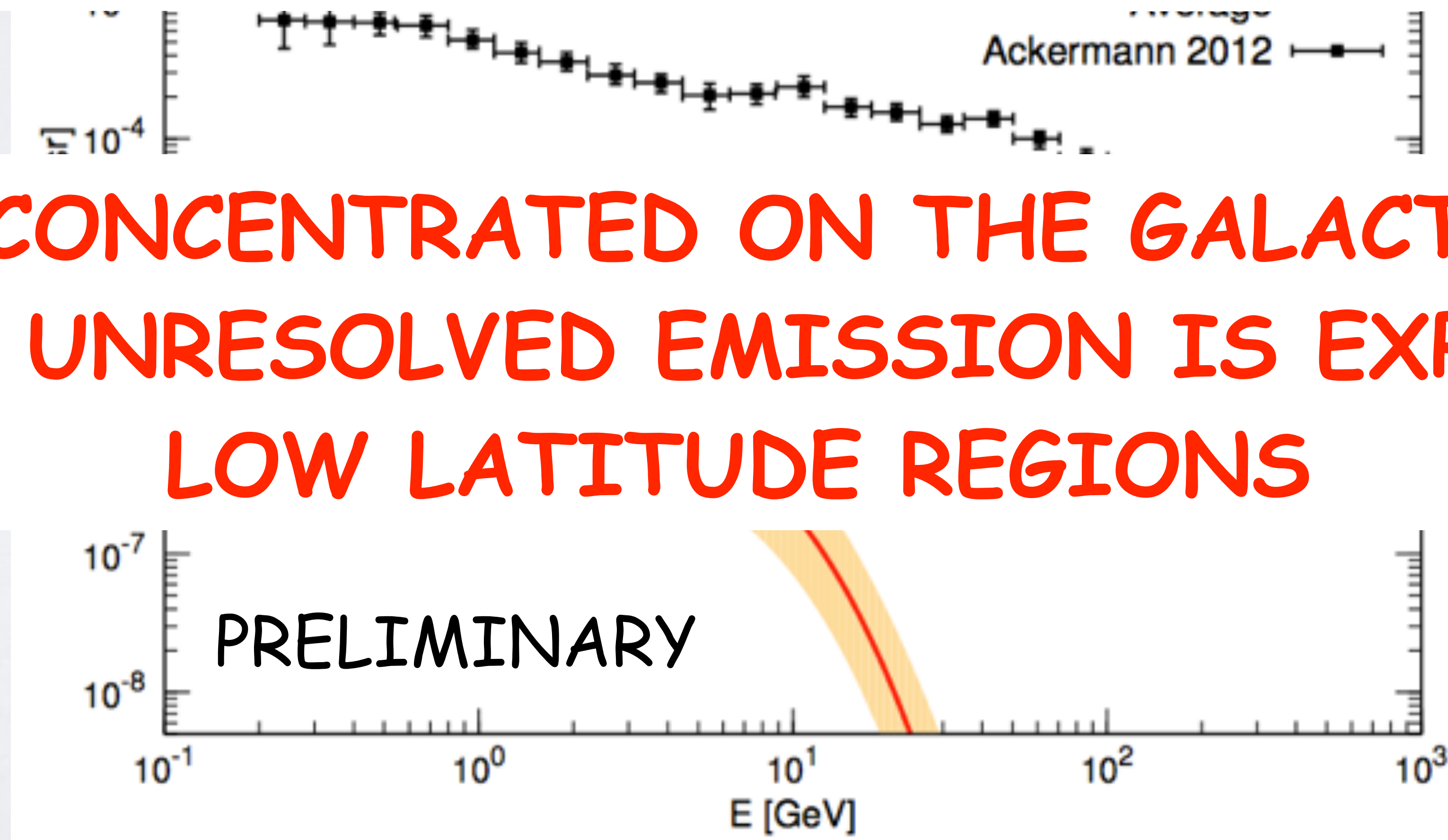

PULSARS CONCENTRATED ON THE GALACTIC PLANE. A LARGER UNRESOLVED EMISSION IS EXPECTED AT LOW LATITUDE REGIONS

DIFFUSE EMISSION IN THE INNER PART OF THE GALAXY

- **Inner galaxy: 10°<|b|<20° and 0<l<360**
- Hooper et al. 2013 derived an excess.
- **Pulsars could account for at most a 5% of the excess in the peak at 2 GeV.**
- MSPs contribution is quite larger than the one of young sources.

- **Galactic center: |b|<3.5° and |l|<3.5°**
- Gordon & Macias 2013 and Abazajian et al. 2014 found and excess in this region.
- Differences in the spectra of the excess are due to different modeling of the ɣ-ray background and template for the point sources.
- **Pulsars and MSPs could contribute for at most a 10% to the excess at the peak.**

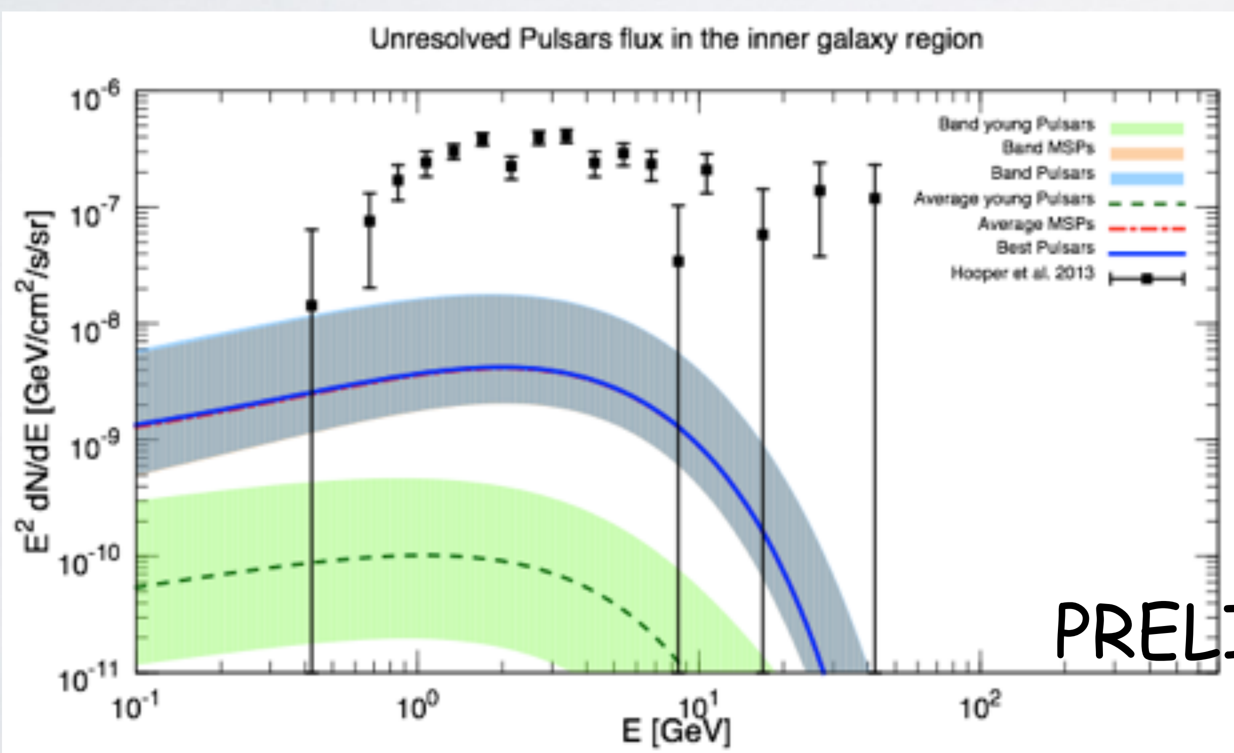

PRELIMINARY

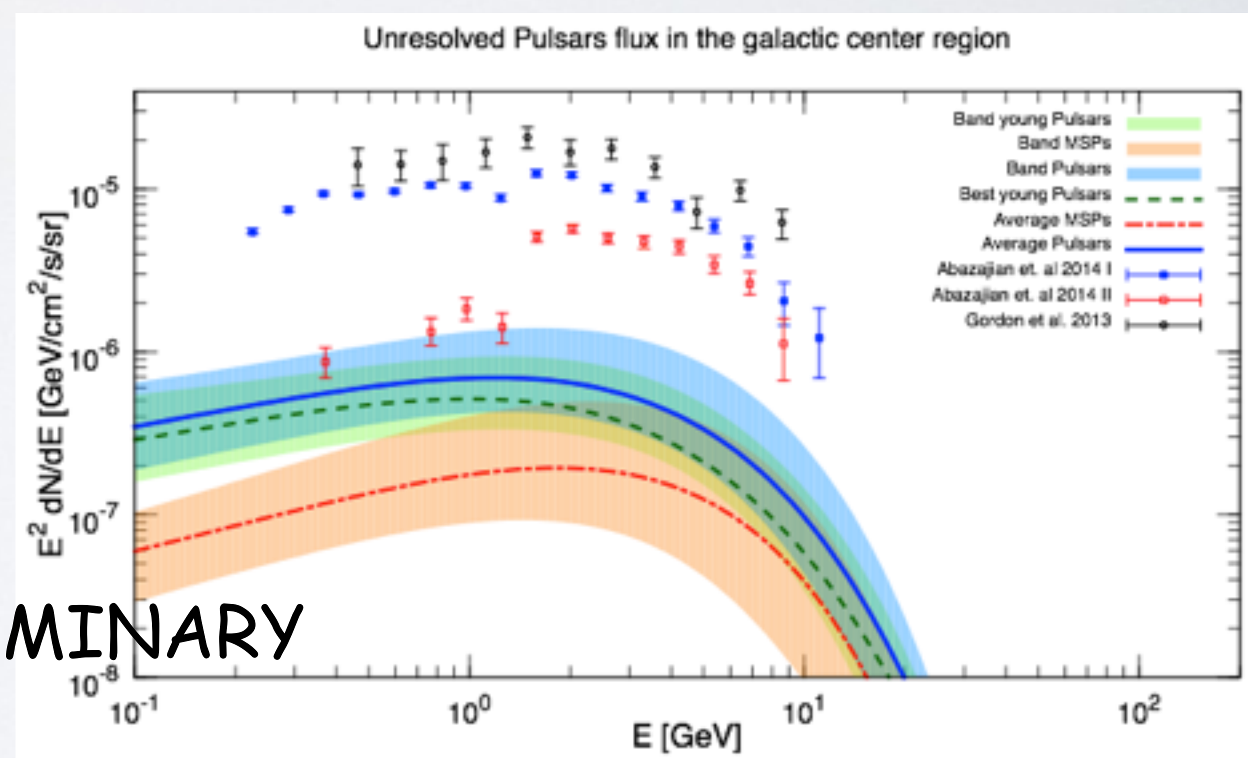

Hooper, D. & Slatyer, T. R. 2013, Physics of the Dark Universe, 2, 118
Gordon, C. & Macias, O. 2013, Phys.Rev., D88, 083521
Abazajian, K. N., Canac, N., Horiuchi, S., & Kaplinghat, M. 2014

UNRESOLVED EMISSION FROM MISALIGNED ACTIVE GALACTIC NUCLEI

Diffuse γ-ray emission from misaligned active galactic nuclei.
M. Di Mauro, F. Calore, F. Donato, M. Ajello, L. Latronico.
arXiv:1304.0908. 2014 ApJ 780 161

MAGN AGN

- MAGN are RG and SSRQ AGN which have a jet orientation misaligned respect to the line of sight ($\varphi > 14°$).
- 15 detected MAGN in the first and the second LAT catalogues. 10 FRI and 5 FRII galaxies (Abdo et al. 2010 ApJ,720,912, Ackermann et al. 2011 ApJ,743,171).

- Luminosity function: number of sources emitting per unit comoving volume, per unit of luminosity.

$$\rho(z, L_\gamma) = \frac{d^2 N}{dV\, dL_\gamma}$$

- Bulk of the radiation is generated via synchrotron self-Compton (SSC) or external inverse Compton (EC) scattering close the center of the source
- ρ_γ derived form the radio luminosity function. We used the total luminosity function given by Willot et al. 2001.

$$\rho_\gamma(L_\gamma, z) = k\ \rho_{r,\mathrm{core}}(L_{r,\mathrm{core}}^{5\mathrm{GHz}}(L_\gamma), z)\frac{d\log L_{r,\mathrm{core}}^{5\mathrm{GHz}}(L_\gamma)}{d\log L_\gamma}$$

RADIO-γ CORRELATION

- In order to find ρ_γ we obtain the correlation between core radio and γ-ray luminosities.

$$\log(L_\gamma) = 2.00 \pm 0.98 + (1.008 \pm 0.025)\log(L^{5\mathrm{GHz}}_{r,\mathrm{core}})$$

- We derive 95% C.L. γ-ray upper limits on a sample (Ghisellini et al. 2005 M. 2005, A&A, 432, 401, Kataoka et al. 2011, ApJ, 740, 29) of undetected MAGN using Fermi-LAT data.

- Correlation is compatible with Fermi-LAT undetected MAGN upper limits.

- We computed a partial correlation analysis and a modified Kendall τ rank correlation test.

- **We concluded the correlation is happening by chance at the 95% C.L.**

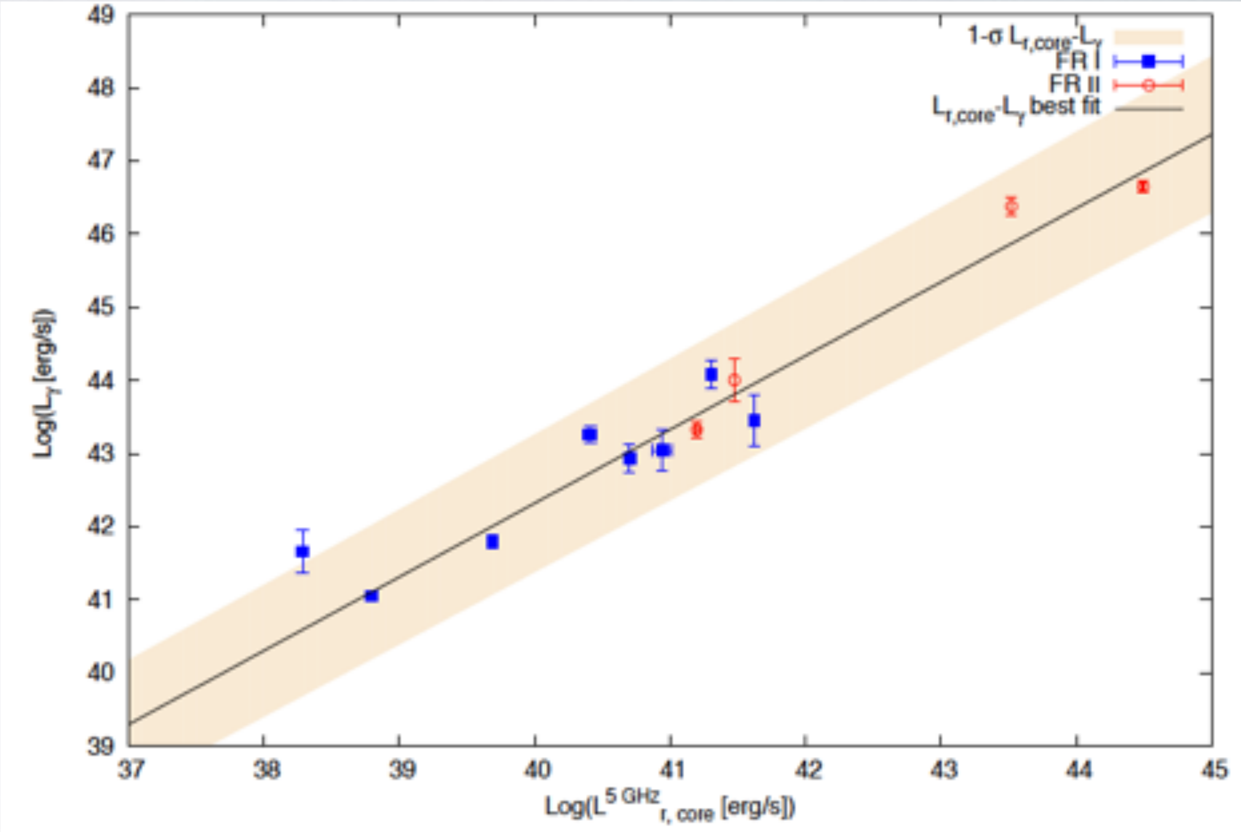

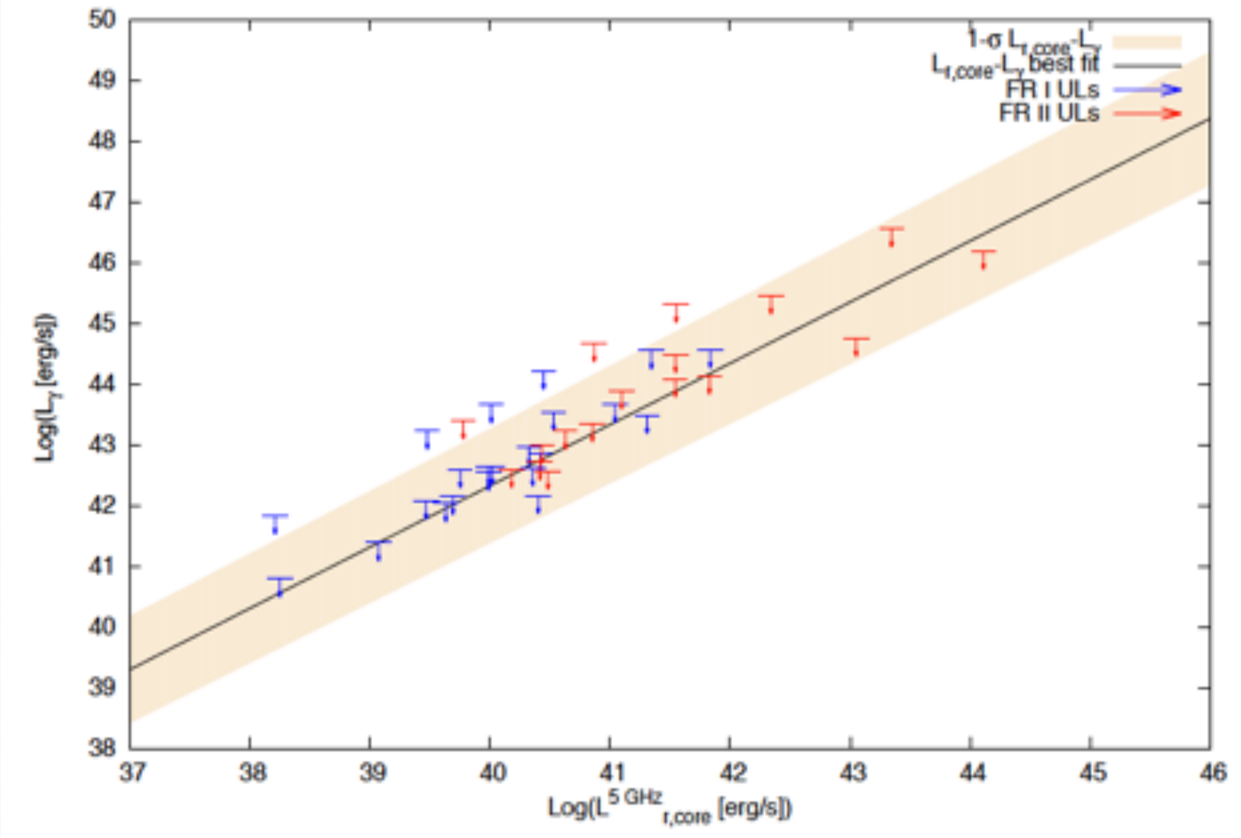

SOURCE COUNT DISTRIBUTION

We derived the experimental source count distribution for the 12 MAGN of our sample and we compared it with the theoretical N count.

$$N_{\rm th}(>F_\gamma) = 4\pi \int_{\Gamma_{max}}^{\Gamma_{min}} \frac{dN}{d\Gamma} d\Gamma \int_0^{z_{max}} \frac{d^2V}{dz d\Omega} dz \int_{L_\gamma(F_\gamma, z, \Gamma)}^{L_\gamma^{max}} \frac{dL_\gamma}{L_\gamma \ln(10)} \rho_\gamma(L_\gamma, z, \Gamma)$$

Green shaded band: k = 1.
Pink band: N(>Fγ) for all the configurations compatible (1σ C.L) with Lγ- Lr,core correlation.
Cyan band: N(>Fγ) for all the configurations in pink band and compatible (1σ C.L.) with experimetal N count.

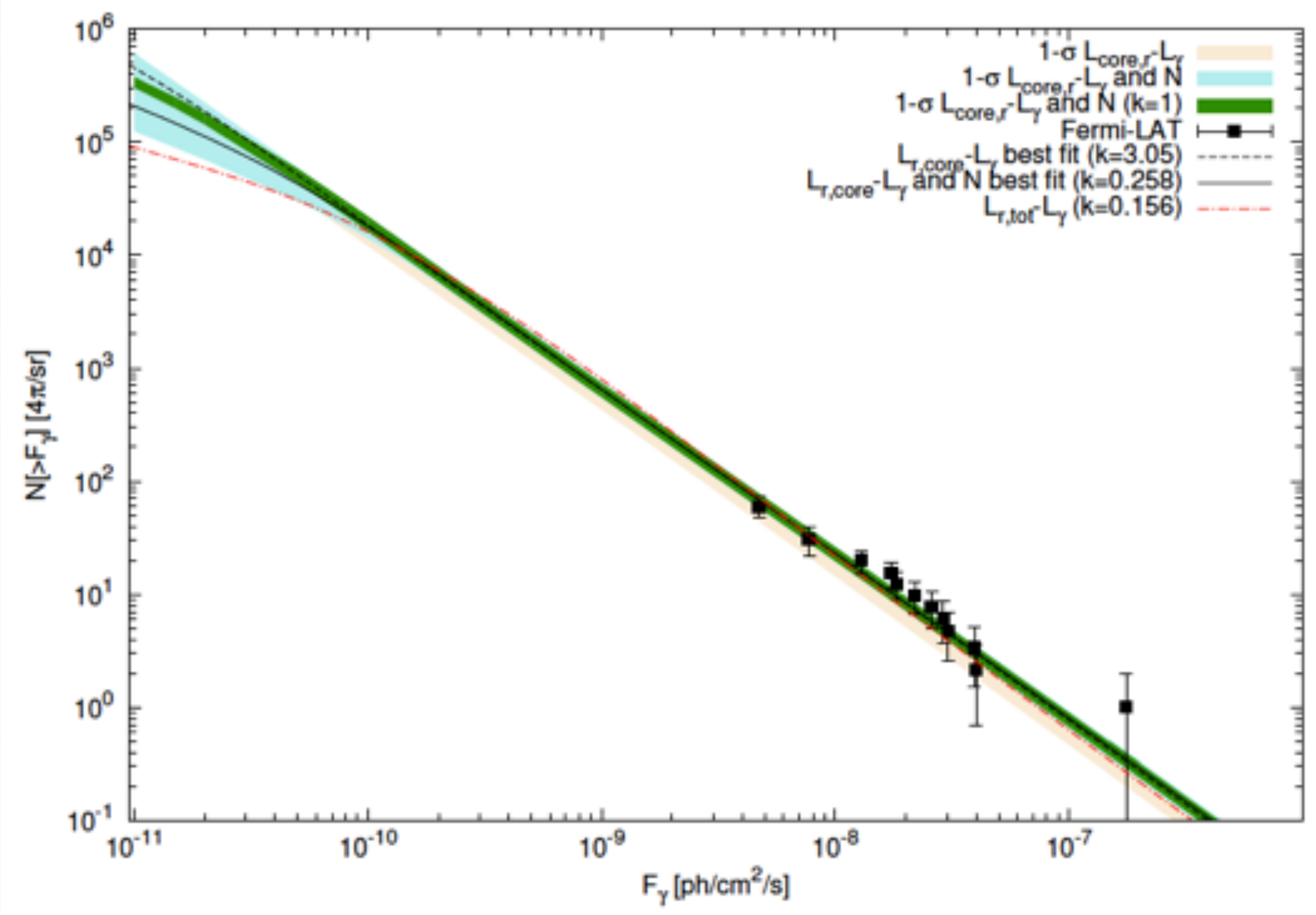

Our model compatible with Fermi-LAT source count distribution.

$$\rho_\gamma(L_\gamma, z) = k\ \rho_{r,\rm core}(L_{r,\rm core}^{\rm 5GHz}(L_\gamma), z) \frac{d \log L_{r,\rm core}^{\rm 5GHz}(L_\gamma)}{d \log L_\gamma}$$

EBL ABSORPTION

High-energy γ-rays (> 20 GeV) propagating in the Universe could be absorbed by the interaction with the extragalactic background light (EBL)

The γ-ray absorption creates e^+e^- pairs, which can scatter off the CMB photons through inverse Compton (IC) yielding a secondary cascade emission at lower γ-ray energies.

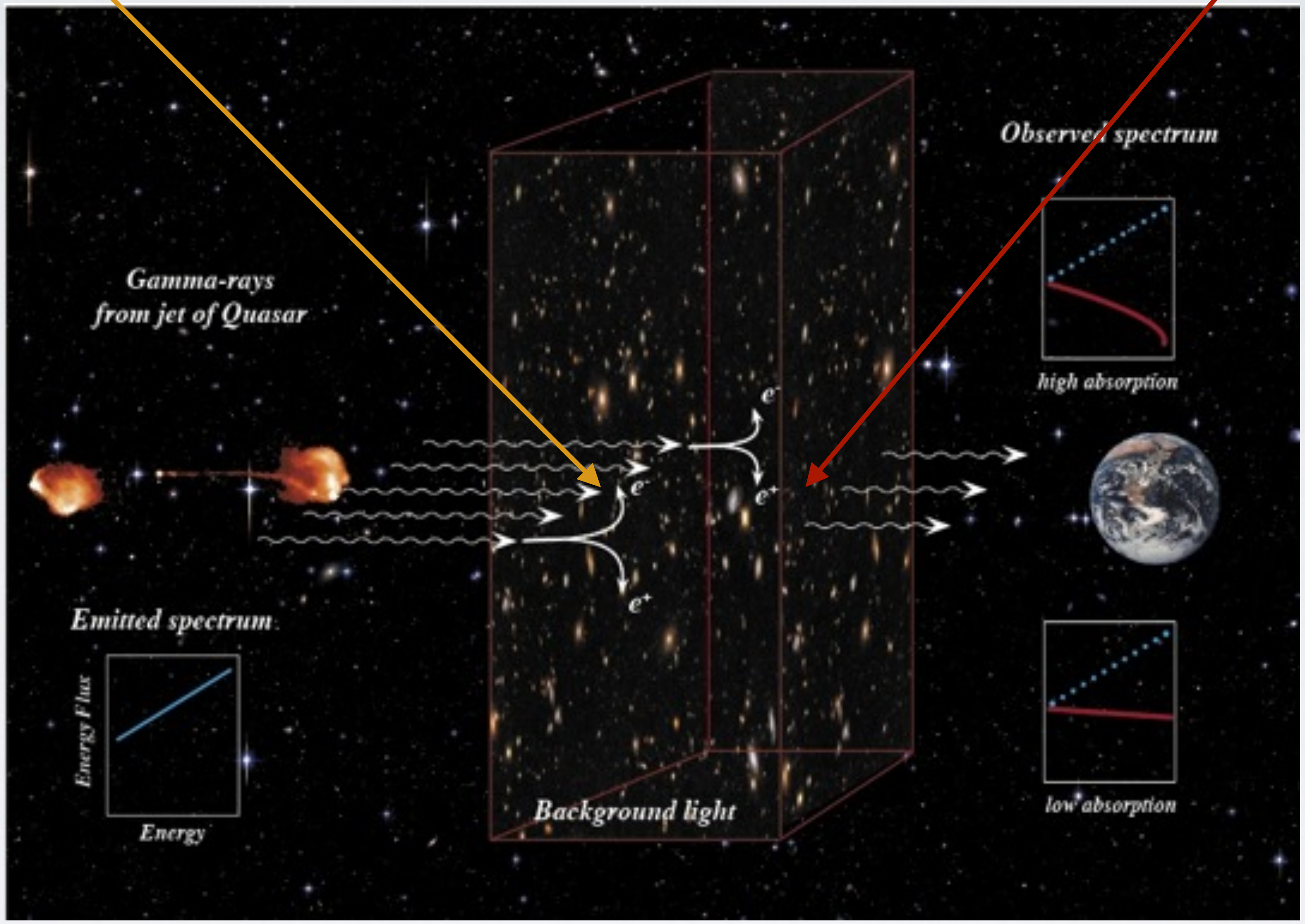

We adopt the attenuation model of Finke et al. (2010).

We checked that using the opacity of Franceschini et al. (2008) or Gilmore et al. (2012) would have a negligible impact on our results.

We include the cascade emission from high-energy γ-rays and accounting for the first generation of electrons produced from the interaction of γ-rays with the EBL.

THE DIFFUSE γ-RAY EMISSION FROM MAGN

- dN/dΓ spectral index distribution
- d2V/dz/dΩ comoving volume

$$\frac{d^2F(\epsilon)}{d\epsilon\, d\Omega} = \int^{\Gamma_{max}} d\Gamma \frac{dN}{d\Gamma} \int^{z_{max}} \frac{d^2V}{dz\, d\Omega} dz \int^{L_{\gamma,max}} \frac{dF_\gamma}{d\epsilon} \quad (23)$$

MAGN POPULATION COULD ACCOUNT A 20/30 % OF THE IGRB SPECTRUM BUT UNCERTAINTIES ARE STILL TOO LARGE!!!!

- **We predict a diffuse γ-ray flux due to MAGN of about $1.6 \cdot 10^{-4}$ MeV cm^{-2} s^{-1} sr^{-1} at 1 GeV.**
- **The uncertainty band is nearly a factor of ten.**
- **At all Fermi-LAT energies, the best fit MAGN contribution is 20%-30% of the IGRB flux.**

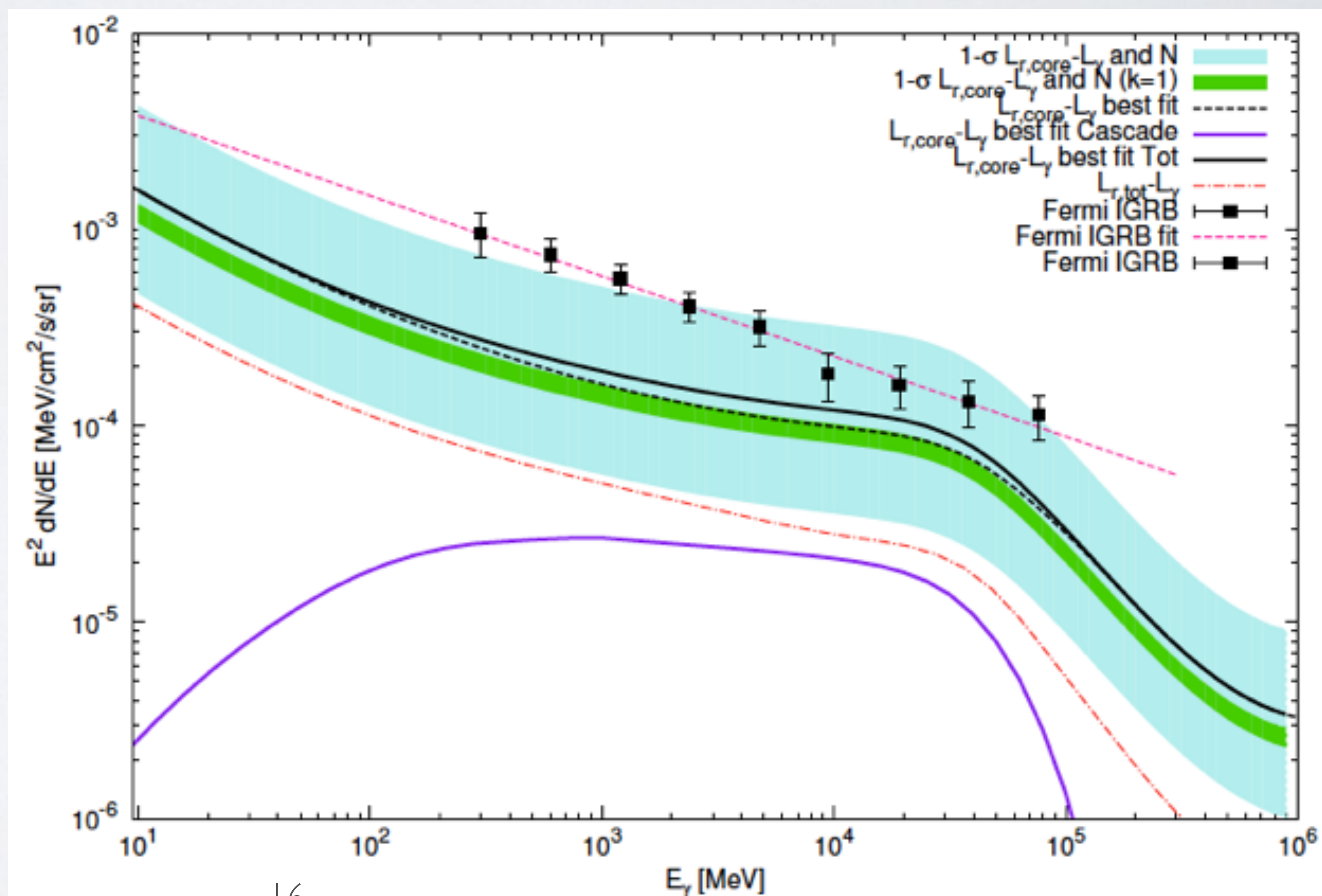

UNRESOLVED EMISSION FROM BL LACERTAE AGN

Diffuse γ-ray emission from BL Lac blazars.
M. Di Mauro, F. Donato, G. Lamanna, D. A. Sanchez, P. D. Serpico.
arXiv:1311.5708. Submitted to APJ.

BLAZARS

- **Flat-spectrum-radio-quasars (FSRQs)** if emission lines and/or the big blue bump are observed.
- **BL Lacertae (BL Lac)** objects if the optical/UV spectrum is dominated by the continuum emission

BLAZAR SEQUENCE

The Spectral Energy Distributions (SEDs) of blazars are characterized by a double peaked luminosity structure.

The low-energy peak is well explained by synchrotron emission from relativistic electrons in a jet closely aligned to the line of sight.

The high energy (hard X-ray and γ-ray) is usually explained as arising from inverse Compton scattering of the same electrons producing the synchrotron emission.

The position of the peak frequency of the first component is used to differentiate among subclasses of BL Lac objects:

- Low-synchrotron-peaked blazar (LSP $\nu_{peak} < 10^{14}$ Hz)
- Intermediate-synchrotron-peaked blazar (ISP 10^{14} Hz $< \nu_{peak} < 10^{15}$ Hz)
- High-synchrotron-peaked peak blazar (HSP $\nu_{peak} > 10^{15}$ Hz).

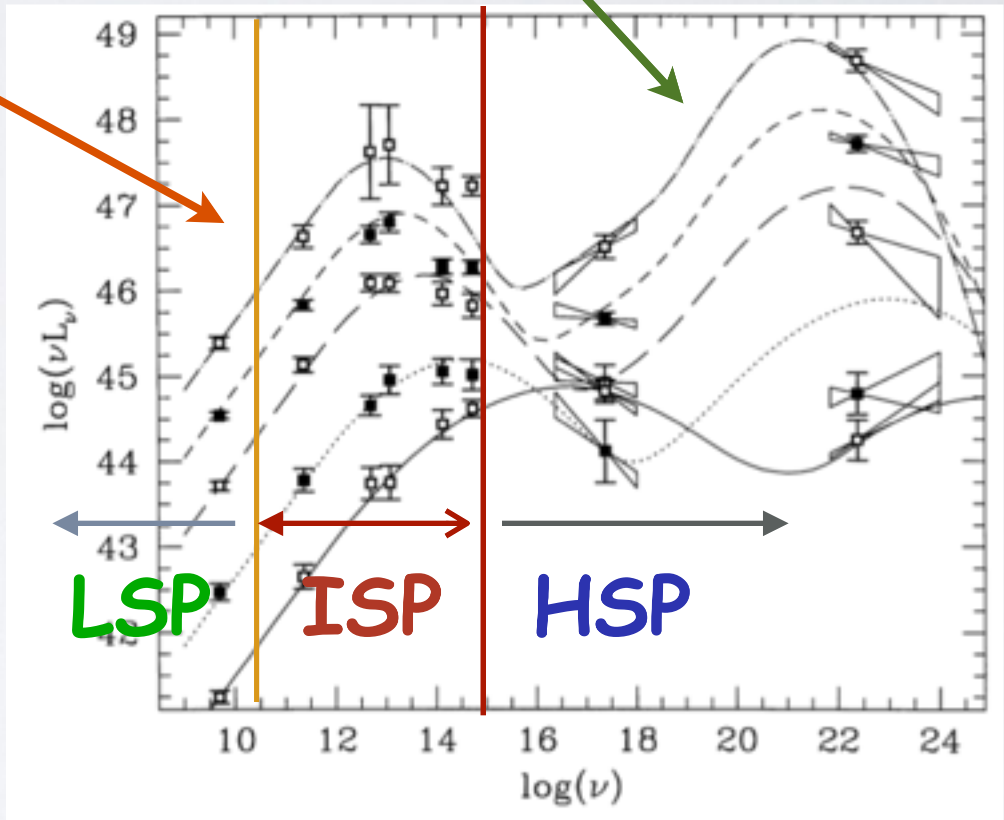

Fossati 1998 1998MNRAS.299..433F

SED ANALYSIS

- We have considered the 2FGL catalogue (Nolan et al. 2012 ApJS 199 31N),
- The first high energy Fermi Catalog (2013arXiv1306.6772T) and
- for H
- We tr
- a sim

THE POWER LAW WITH THE EXPONENTIAL CUT OFF IS THE BEST MODEL TO FIT THE SED DATA

- a log-parabola and

$$\frac{dN}{dE} = K' \left(\frac{E}{E_0}\right)^{-\alpha-\beta \log\left(\frac{E}{E_0}\right)}$$

- simple power law + exponential cut off

$$\frac{dN}{dE} = K'' \left(\frac{E}{E_0}\right)^{-\Gamma_{\rm cut}} \exp\left(-\frac{E}{E_{\rm cut}}\right)$$

- All spectra data are corrected for the EBL absorption.

LSP/ISP/HSP

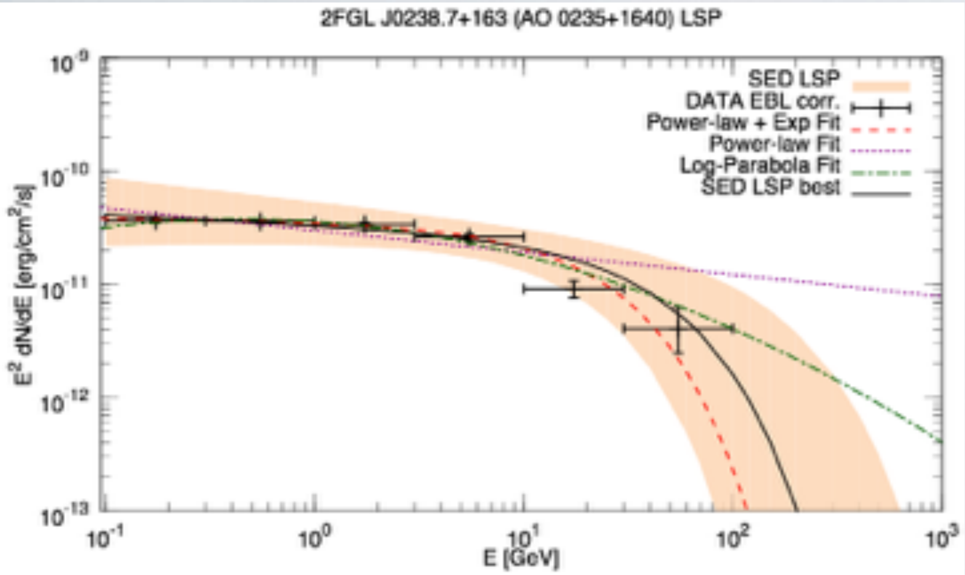

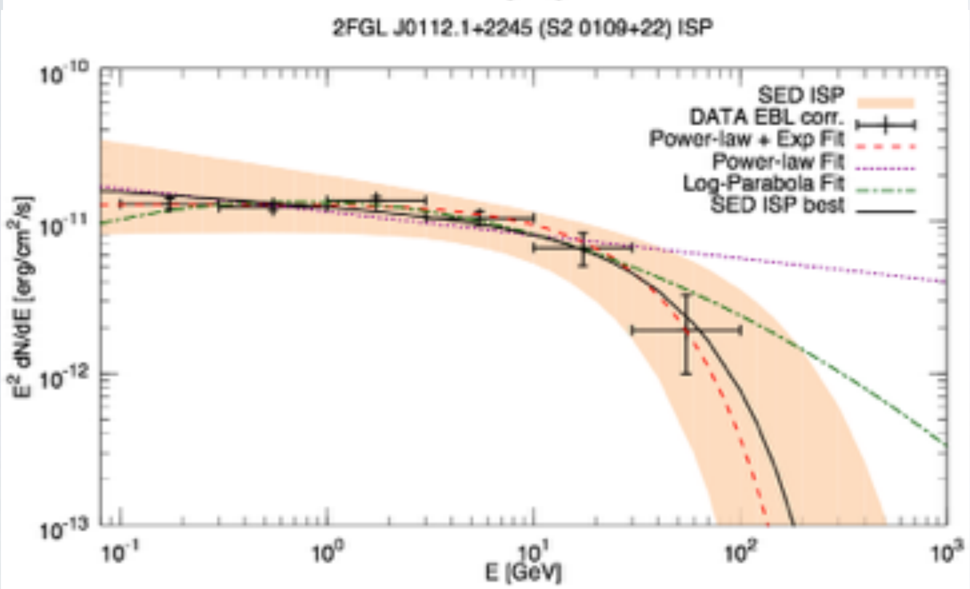

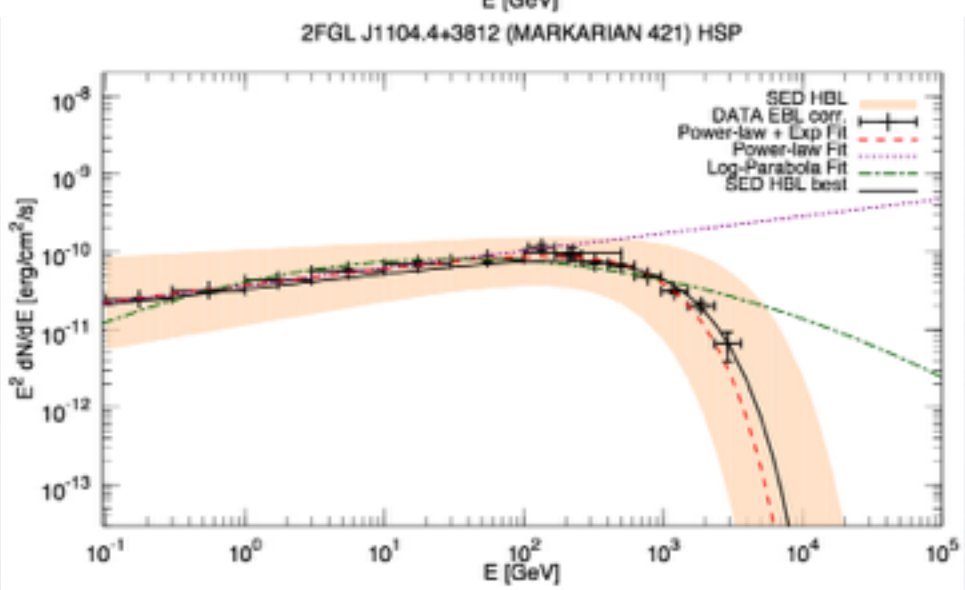

- LSP/ISP/HSP in the 2FGL, 1FHL and TeV catalogs with a SED classification, a measured redshift and with $F_\gamma > 1.5 \cdot 10^{-8}$ photons cm^{-2} s^{-1}
- The sample of LSP/ISP/HSP is made of 19/21/23 sources.

- LSP: $\Gamma = 2.08 \pm 0.13$ and Ecut $= 34^{+85}_{-20}$ GeV
- ISP: $\Gamma = 2.07 \pm 0.14$ and Ecut $= 40^{+80}_{-20}$ GeV
- **HSP: $\Gamma = 1.86 \pm 0.16$ and Ecut $= 910^{+1100}_{-450}$ GeV**

→ **LISP: $\Gamma = 2.05 \pm 0.16$ and Ecut $= 36^{+100}_{-30}$ GeV**

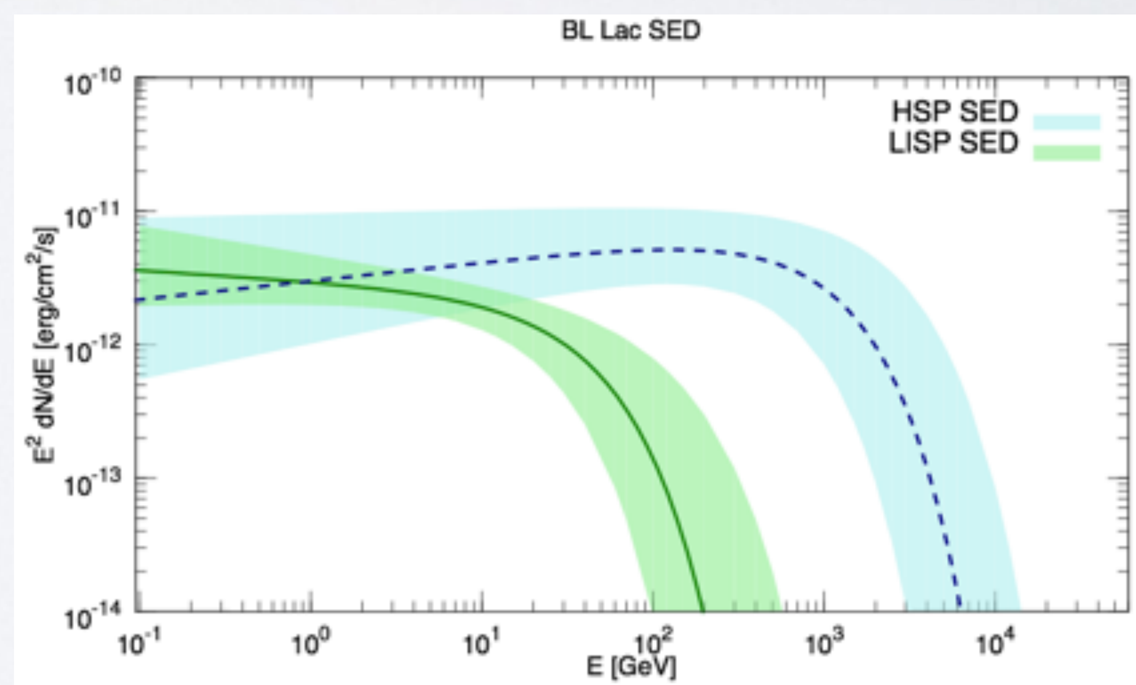

γ-RAY LUMINOSITY FUNCTION

- We have considered the 2FGL catalog.
- Taken into account all the BL Lac with a measured redshift, a SED classification.
- The sample is composed by 80 HSP, 34 ISP and 34 LSP.
- The space density of BL Lac is defined by:

$$\Theta_\gamma(z,\Gamma,L_\gamma) = \frac{d^3N}{dz\,d\Gamma\,dL_\gamma} = \frac{d^2N}{dV\,dL_\gamma}\frac{dV}{dz}\frac{dN}{d\Gamma} = \rho_\gamma(z,L_\gamma)\frac{dV}{dz}\frac{dN}{d\Gamma}$$

- In order to find ρ we take into account three theoretical functions: the **Pure Luminosity Evolution** (PLE, Hasinger et al. 2005; Ueda et al. 2003), the **Luminosity-dependent Density Evolution** (LDDE, Ueda et al. 2003) and the **Steep-Spectrum Radio Sources** (SSRS, Willott et al. 2001) models.
- In order to find the best fit values of the luminosity function parameters we fit the experimental redshift, γ-

LDDE the best model to represent the luminosity function.

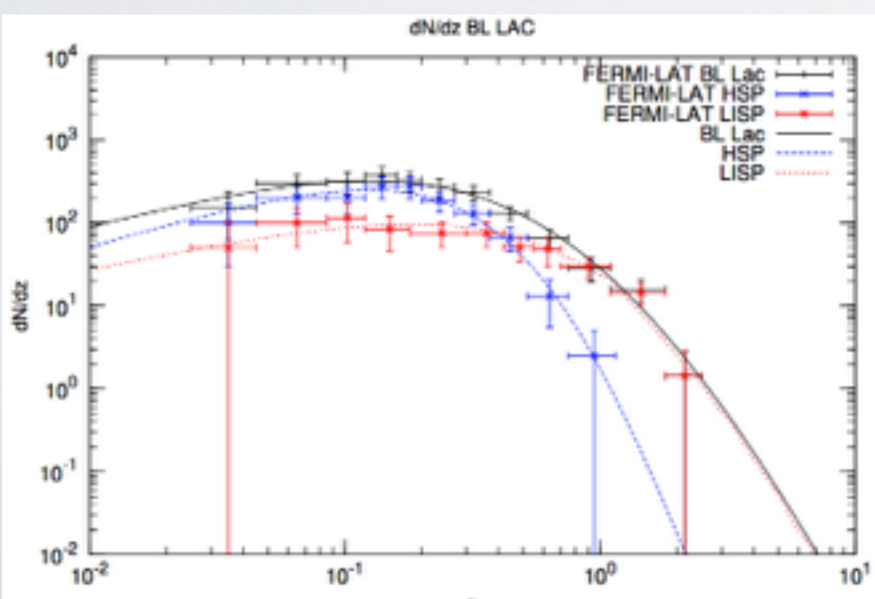

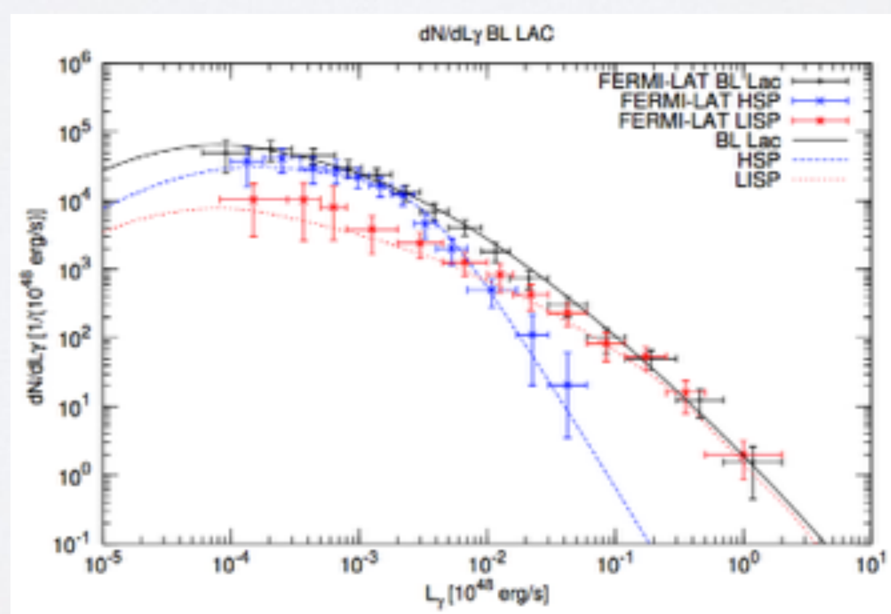

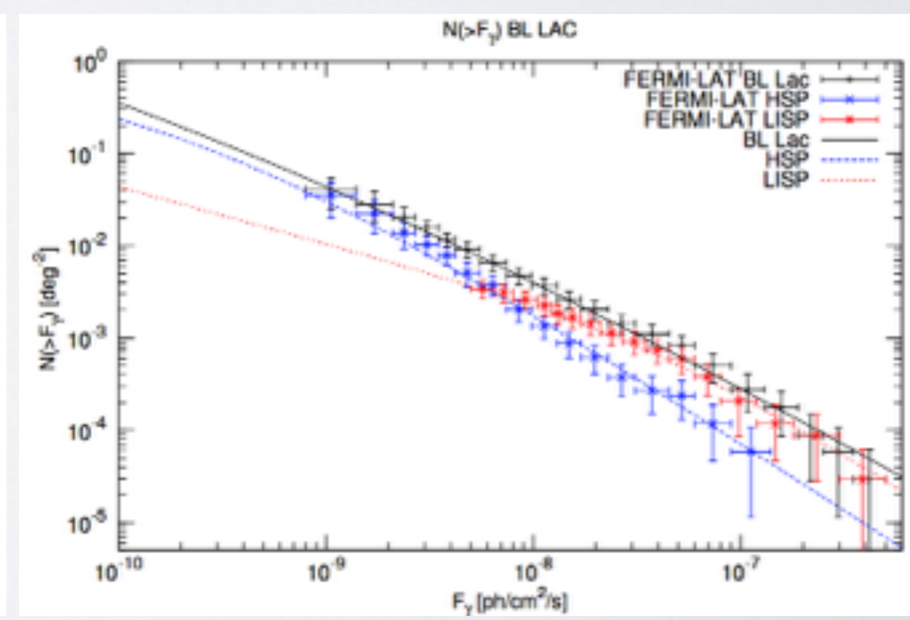

DIFFUSE EMISSION FROM BL LAC

- We compute the diffuse γ-ray emission from unresolved BL Lac both when treated as a unique population, as well as considering the two sub-populations of LISP and HSP separately.
- The high energy LISP and HSP flux is shaped by the cut-off of the SEDs, while for the case of the BL Lacs treated as unique population only the γ-rays EBL absorption intervenes in softening the spectrum
- The contribution from the cascade emission amounts to no more than ~30% of the primary flux, and additionally in the GeV range where the BL Lac contribution to the IGRB is anyway subdominant.

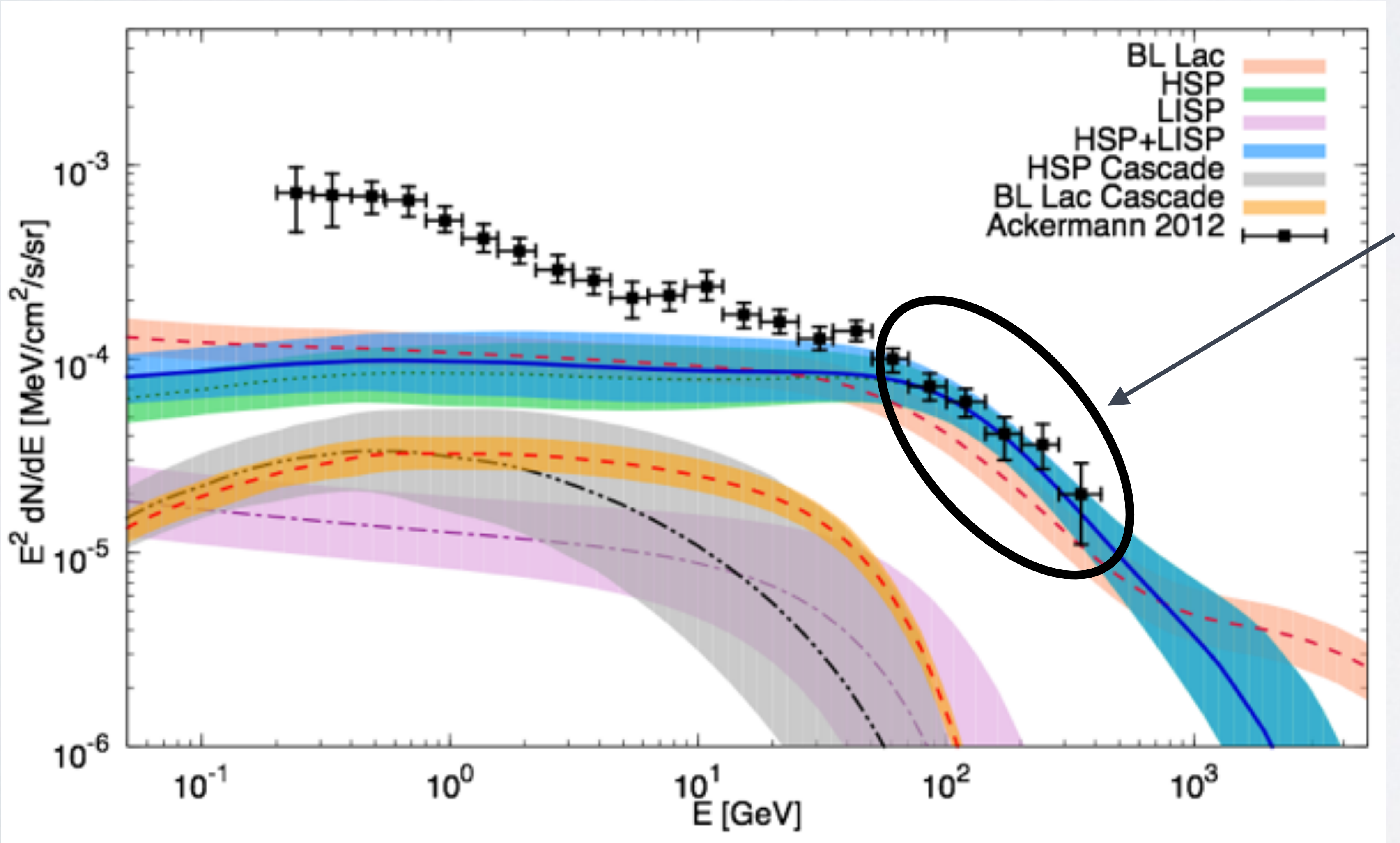

The estimated contribution to the measured IGRB between 100 MeV and 100 GeV amounts merely to ~11% of the Fermi-LAT data.

Our best estimation seems to fully account for the measured IGRB at Eγ >50 GeV!!!!

COMPOSITION OF […]RB

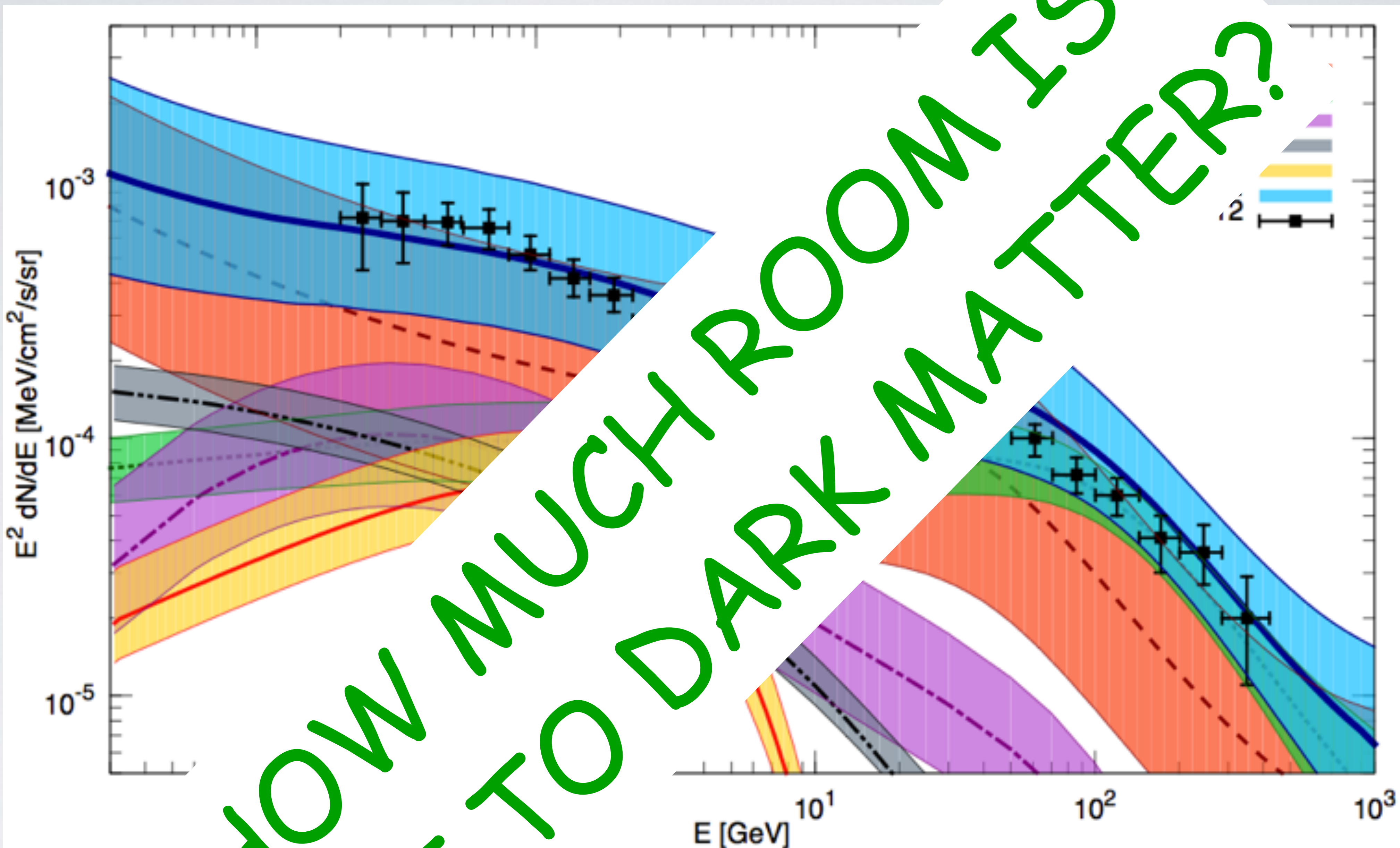

HOW MUCH ROOM IS LEFT TO DARK MATTER?

The sum of th[…] emission from unresolved MSP, SF, FSRQ, MAGN and BL Lac sources […] account from 45% up to 100% to the measured IGRB in the range 200 MeV - 400 GeV.

DARK MATTER ANNIHILATION CONSTRAINTS

Constraining dark matter annihilation with the isotropic γ-ray background: updated limits and future potential.
Torsten Bringmann, Francesca Calore, Mattia Di Mauro, Fiorenza Donato. arXiv:1303.3284. Accepted in PRD.

γ-RAYS FROM GALACTIC DARK MATTER

$$\Phi_\gamma(E_\gamma, \psi) = \frac{1}{4\pi} \frac{\langle \sigma v \rangle}{m_\chi^2} \frac{dN_\gamma}{dE_\gamma} \frac{1}{2} I(\psi)$$

- dN/dE_γ: photon spectrum from Prompt and Inverse Compton (IC) emission.
- $I(\psi)$: geometrical factor for Burkert profile.

$$I(\psi) = \int_{l.o.s.} \rho^2(r(\lambda, \psi)) d\lambda$$

- $\langle\sigma v\rangle$: annihilation DM cross section.
- M_X: DM mass
- $\rho_\odot$: local DM density: 0.4 GeV/cm^3.
- $r_\odot$ Sun-Earth distance: 8.33 kpc

bb channel $\langle\sigma v\rangle$ = 2 10^{-24} cm^3/s M_X = 1 TeV

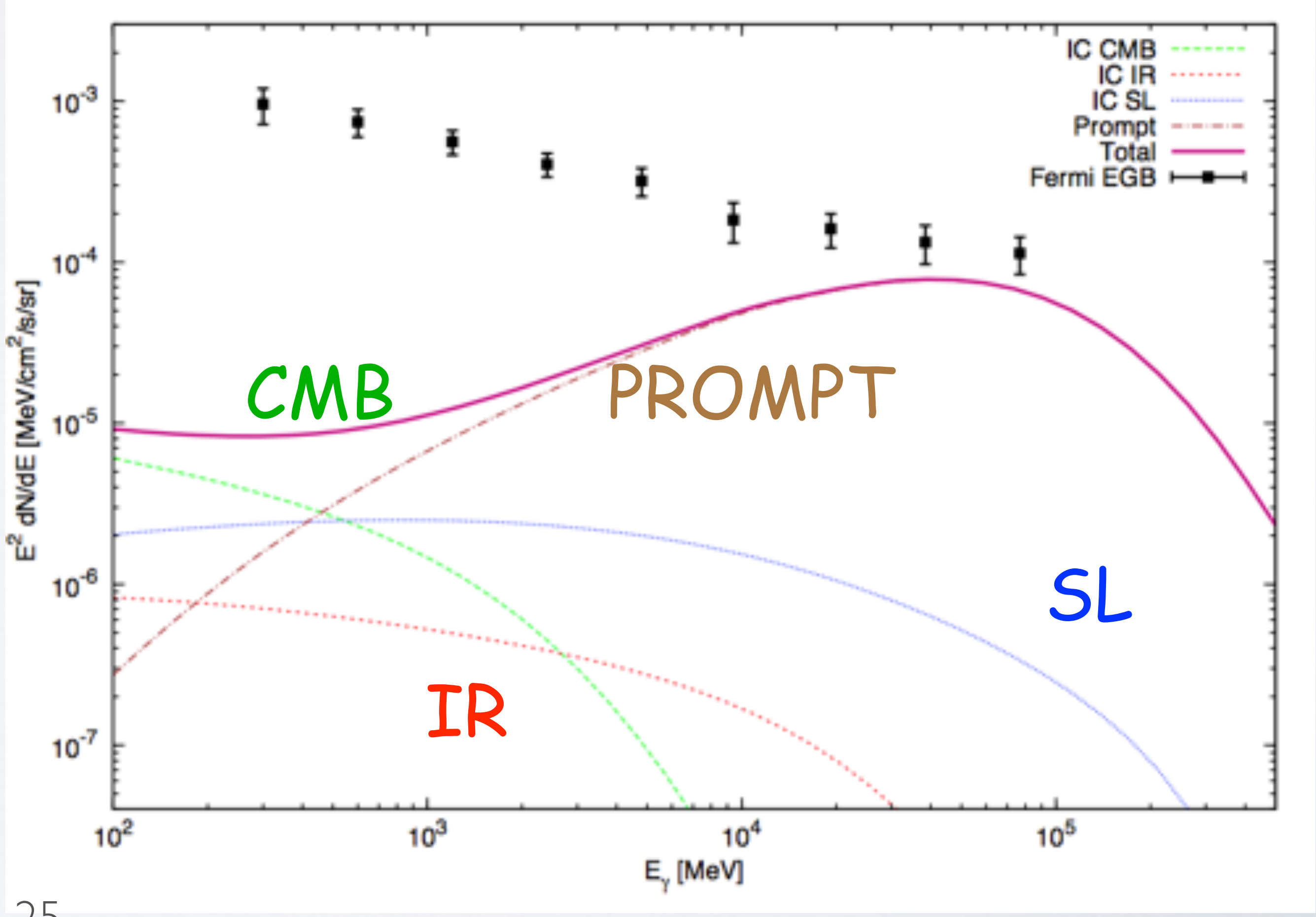

H. Bengtsson, P. Salati, and J. Silk, Nuclear Phys. B 346, 129 (1990).
L. Bergstrom, P. Ullio, and J. H. Buckley, Astropart. Phys. **9**, 137 (1998), 9712318.
A. Bottino, F. Donato, N. Fornengo, and S. Scopel, Phys. Rev. D 70, 015005 (2004), 0401186.

PROCEDURE

- We derive conservative limits on $\langle\sigma v\rangle$ by requiring that the total γ-ray flux does not exceed any of the Fermi-LAT data points (Abdo et al., Phys. Rev. Lett. 104) by more than nσ.
- We have considered four different parametrization for the background:
- **Minimal contribution (2σ)**
- **best fit contribution (2σ)**
- **high background one with 60% of maximal contribution from MAGN (2σ).**
- **and two with 85% of maximal contribution from MAGN (3σ).**
- Take into account the γ-rays produced through IC scattering is significant for leptons channels.

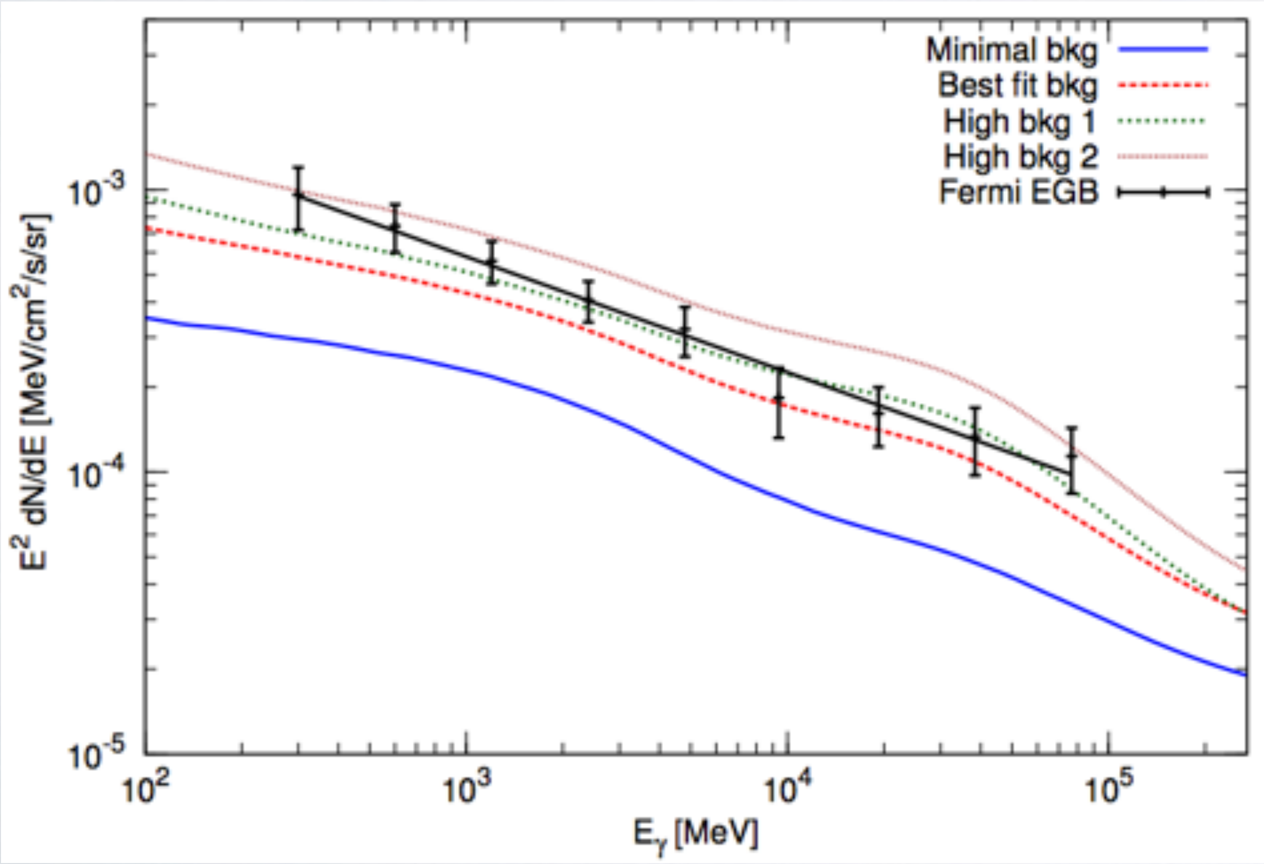

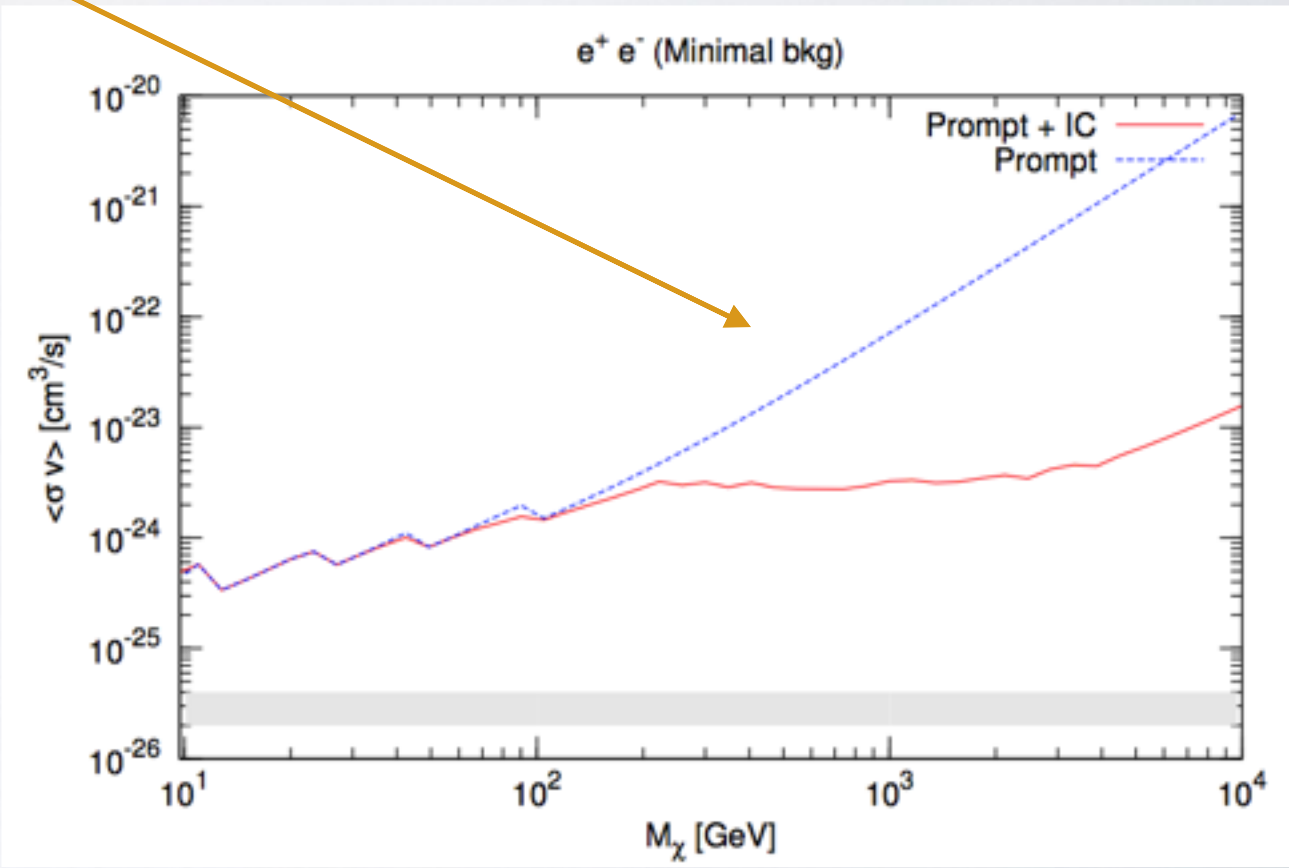

DM CONSTRAINTS

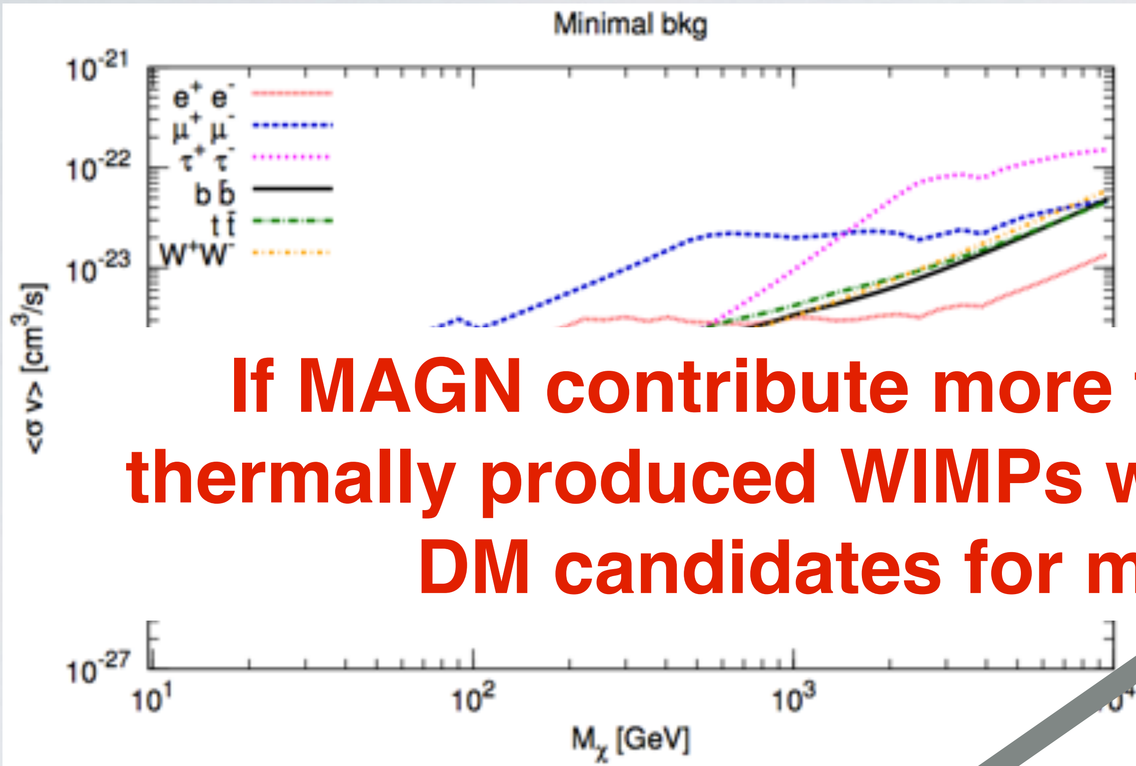

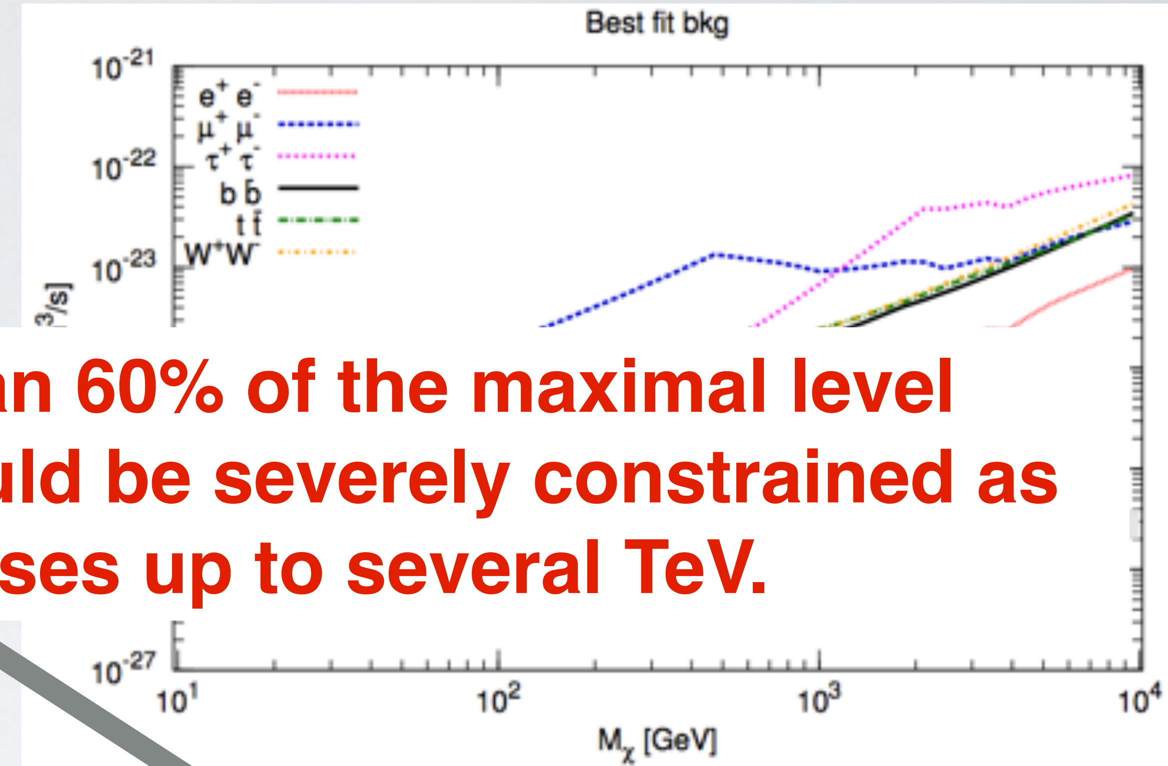

If MAGN contribute more than 60% of the maximal level thermally produced WIMPs would be severely constrained as DM candidates for masses up to several TeV.

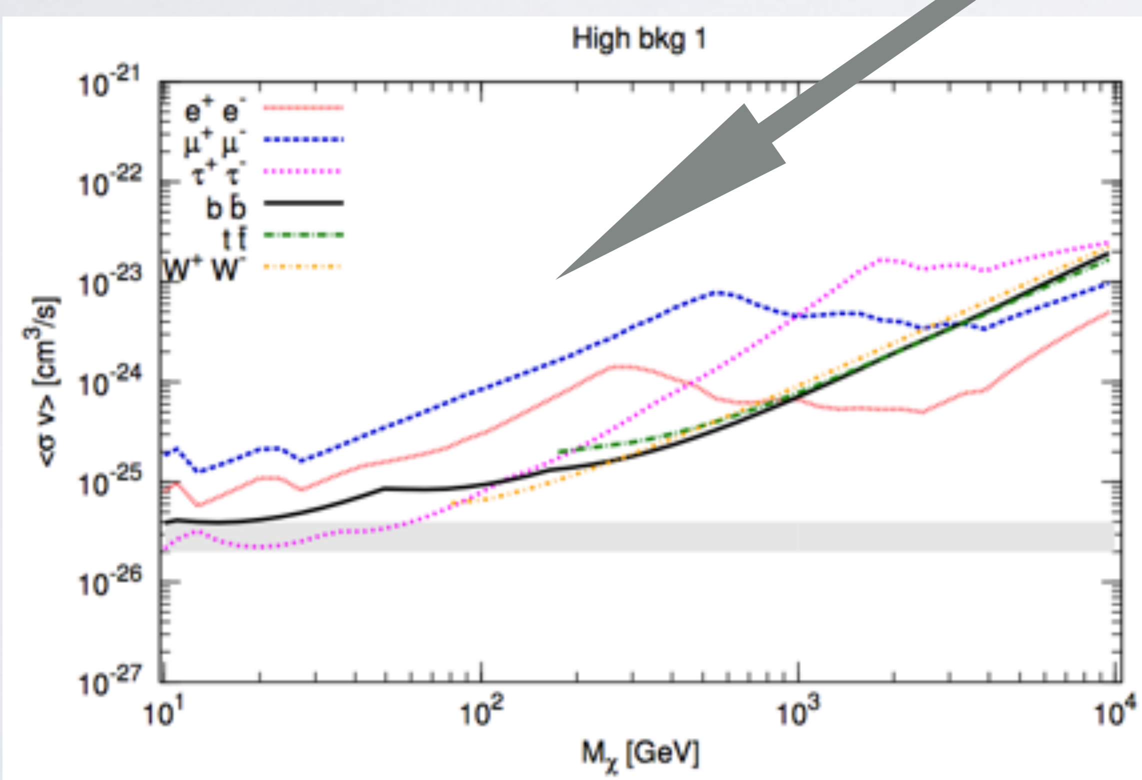

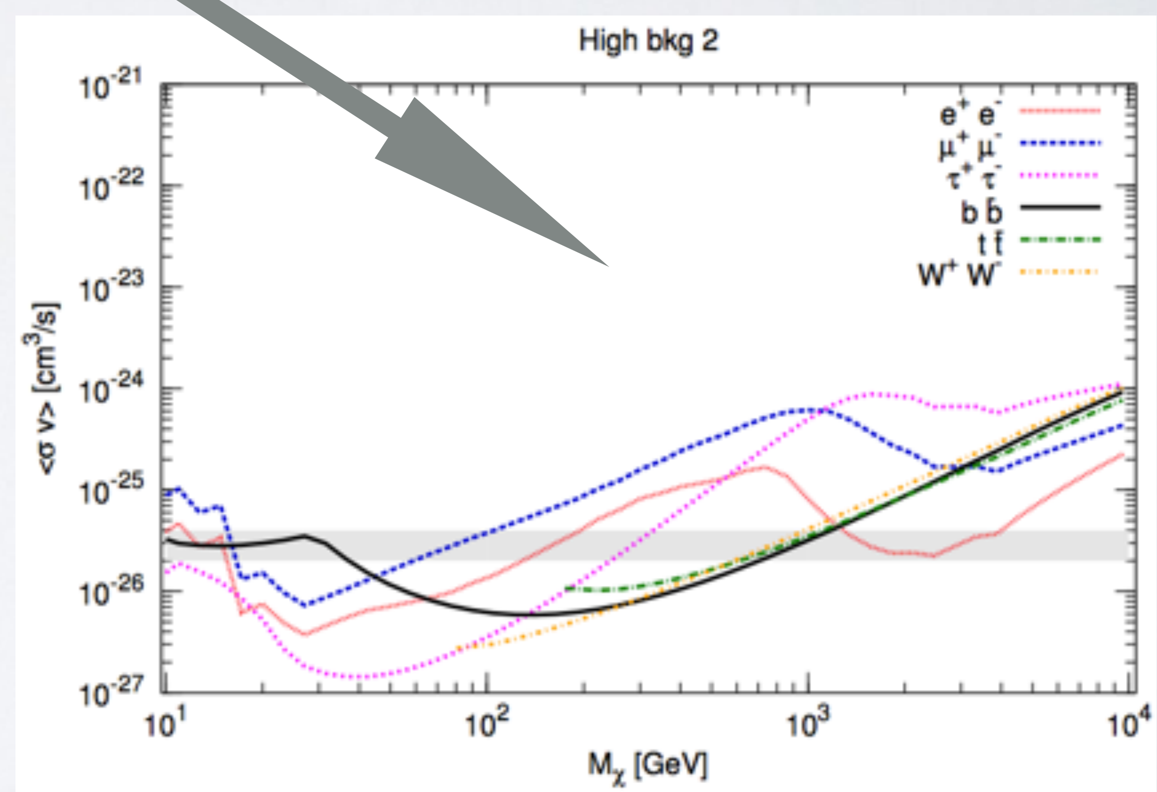

COMPARISON WITH OTHER DM CONSTRAINTS

- Analysis of the diffuse gamma-ray emission in the Milky Way Halo region modeling the foreground astrophysical diffuse emission using the GALPROP code.
- In ... cor
- Cor ... x ma ... gar

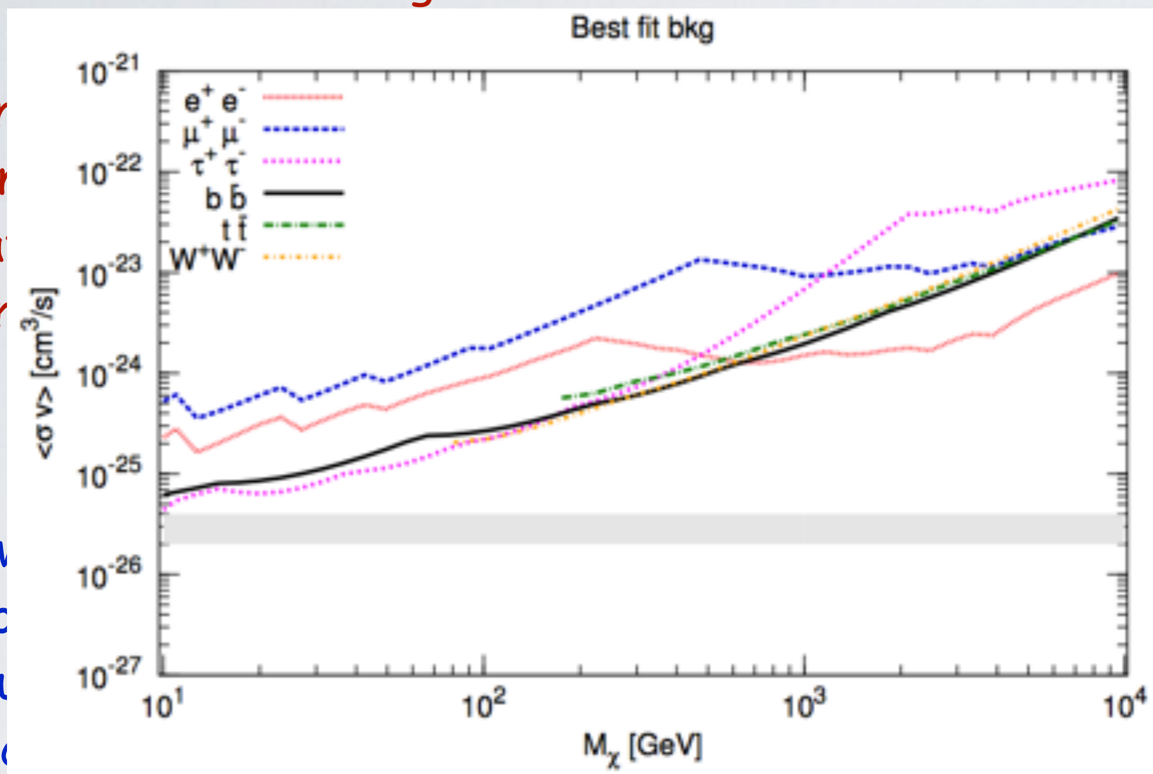

- Dw... do...
- Du... l la... be among the most promising targets for the indirect detection of dark matter.
- None of the dwarf galaxies are signicantly detected in rays, and they present gamma-ray flux upper limits between 500MeV and 500 GeV.

M. Ackermann et al 2013

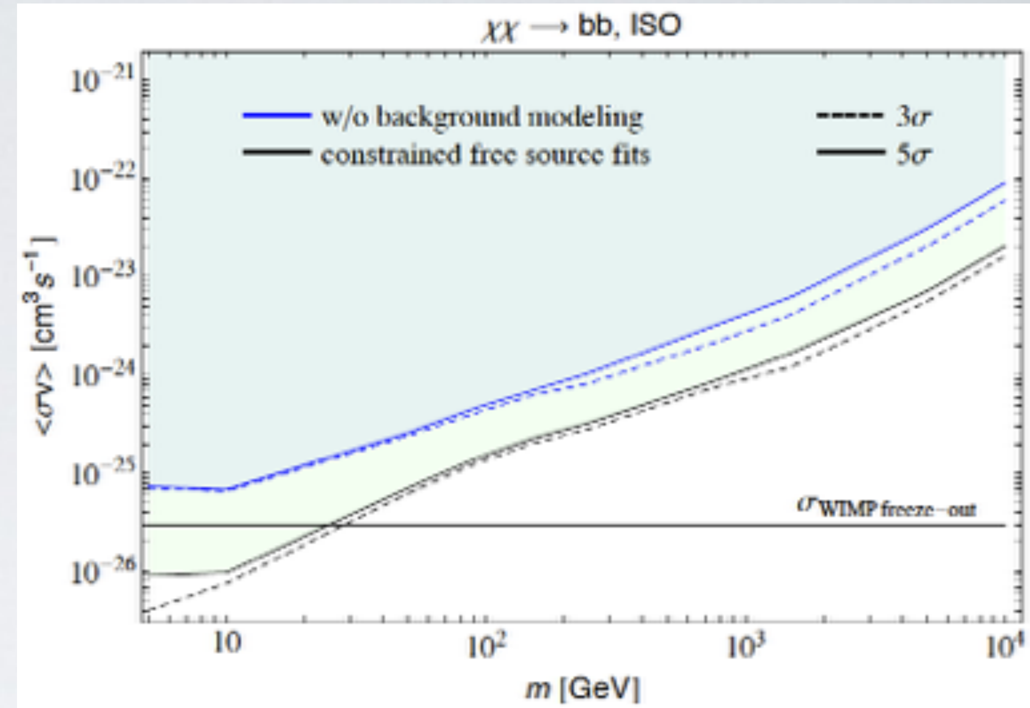

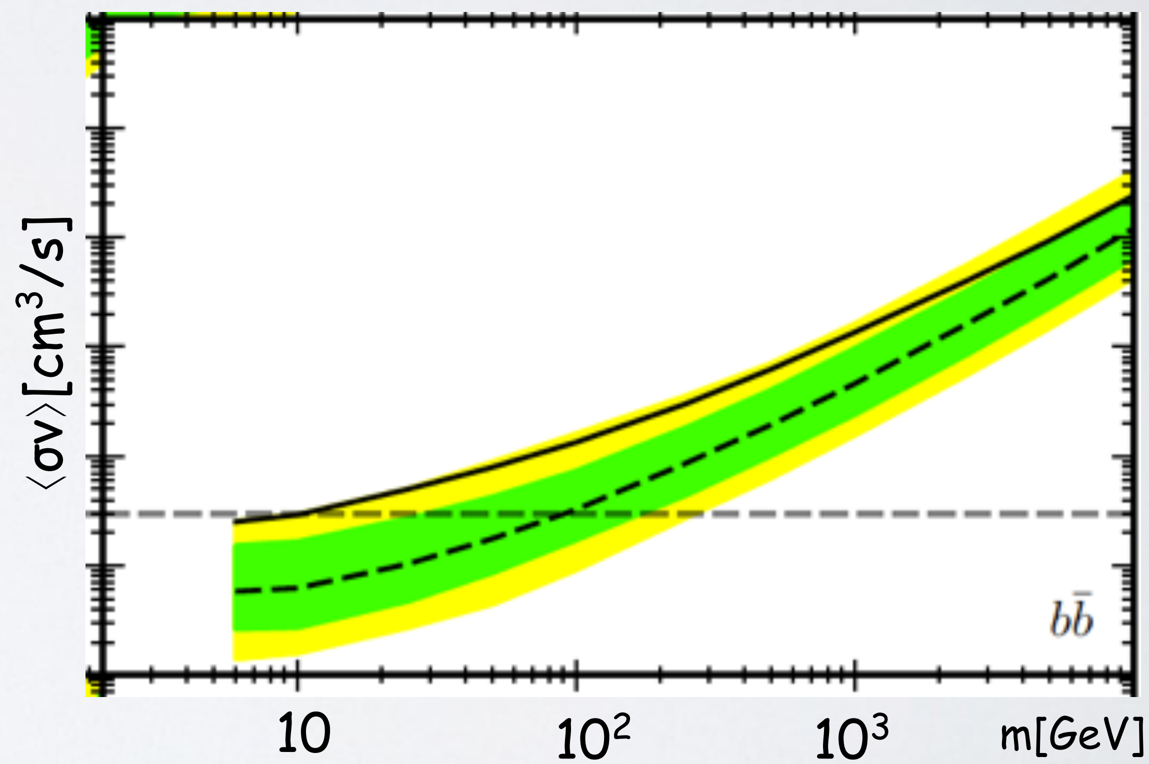

The IGRB has the potential to be one of the most competitive future ways to test the DM WIMP hypothesis, once the present uncertainties are even slightly reduced.

CONCLUSIONS

- UNRESOLVED EMISSION FROM PULSARS IS NEGLIGIBLE AT HIGH LATITUDE (b>10) AND IT IS AT MOST A 10% IN THE INNER PART OF THE GALAXY.
- MAGN POPULATION COULD EXPLAIN A REMARKABLE FRACTION OF THE IGRB BUT THE UNCERTAINTIES ARE STILL TOO LARGE.
- BLLAC COULD EXPLAIN THE DECREASING OF THE IGRB SHAPE AT ENERGIES LARGER THAN 100 GeV.
- IF MAGN CONTRIBUTE MORE THAN 60% OF THE MAXIMAL CONTRIBUTION THERMALLY PRODUCED WIMPs WOULD BE SEVERELY CONSTRAINED AS DM CANDIDATES.

THANK YOU!!

Fiorenza Donato

Dipartimento di Fisica,
Università di Torino,
INFN Torino

Pasquale Dario Serpico

Laboratoire d' Annecy-le-Vieux
de Physique des Particules
(LAPP), Univ. de Savoie,

Luca Latronico

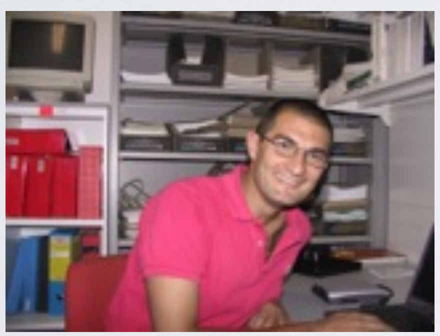

INFN Torino

1) Diffuse γ-ray emission from misaligned active galactic nuclei. M. Di Mauro, F. Calore, F. Donato, M. Ajello, L. Latronico. Astrophysical Journal 780 (2014) 161. arXiv:1304.0908.

2) Diffuse γ-ray emission from BL Lac blazars. M. Di Mauro, F. Donato, G. Lamanna, D. A. Sanchez, P. D. Serpico. arXiv:1311.5708. Submitted to the Astrophysical Journal.

3) Constraining dark matter annihilation with the isotropic γ-ray background: updated limits and future potential. Torsten Bringmann, Francesca Calore, Mattia Di Mauro, Fiorenza Donato. Physical Review D 89,023012 (2014). arXiv:1303.3284

4) Diffuse γ-ray emission from misaligned active galactic nuclei. M. Di Mauro, F. Calore, F. Donato. In preparation.

Giovanni Lamanna

Laboratoire d' Annecy-le-Vieux de Physique des Particules (LAPP), Univ. de Savoie,

Torsten Bringmann

Department of Physics,
University of Oslo

Francesca Calore

GRAPPA Institute,
University of Amsterdam

Marco Ajello

Space Sciences Laboratory, University of California, Berkeley,

BACKGROUND

EXPERIMENTAL BIAS IN SPATIAL DISTRIBUTION

r DISTRIBUTION

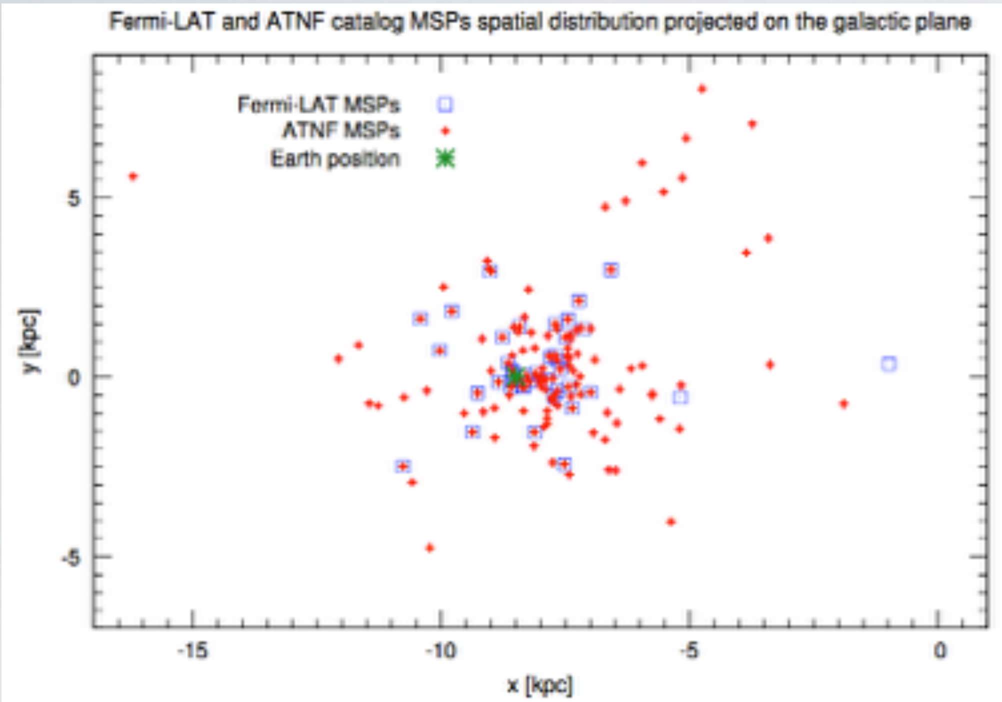

- Radial distribution peaked at 7.5 kpc.
- Models of birth and evolution of radio Pulsars (Lorimer et al. 2006; Faucher-Giguere &Kaspi2006): Pulsars peaked at about 3-4 kpc
- MSPs are old sources: the position uncorrelated with the birth position.
- For this reason, the radial distribution is usually centered in the galactic center ⟨r⟩ = 0 kpc

$$\rho(r, z) \propto \exp\left(-\frac{r^2}{2\sigma_r^2} - \frac{|z|}{z_0}\right)$$

z DISTRIBUTION

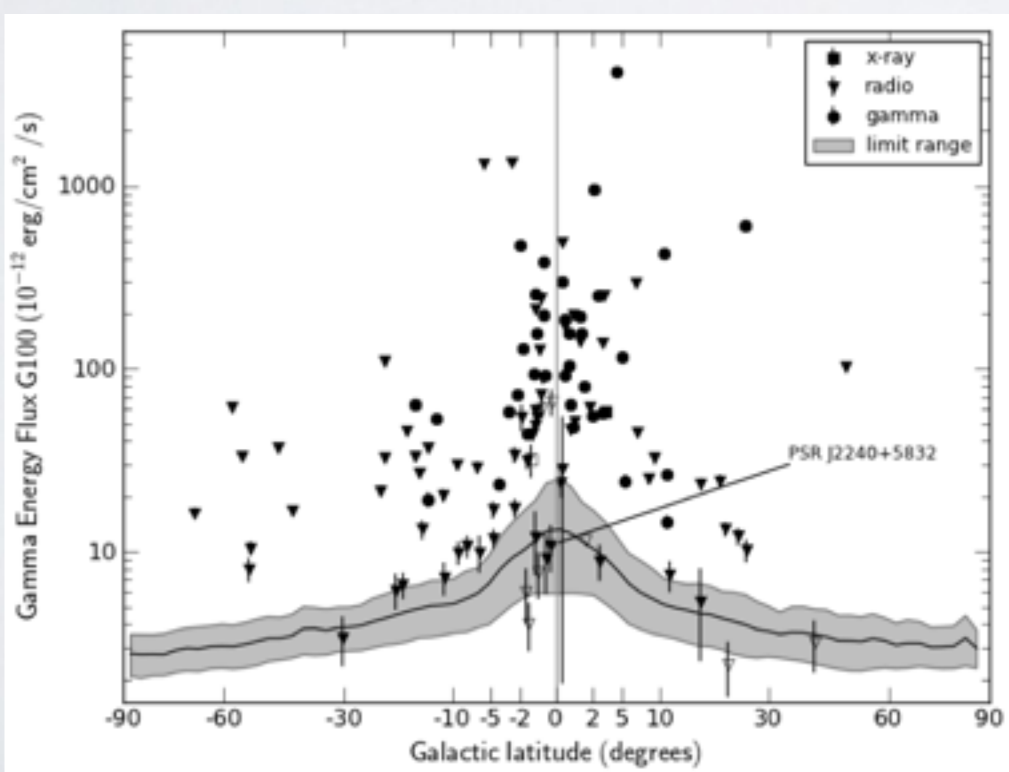

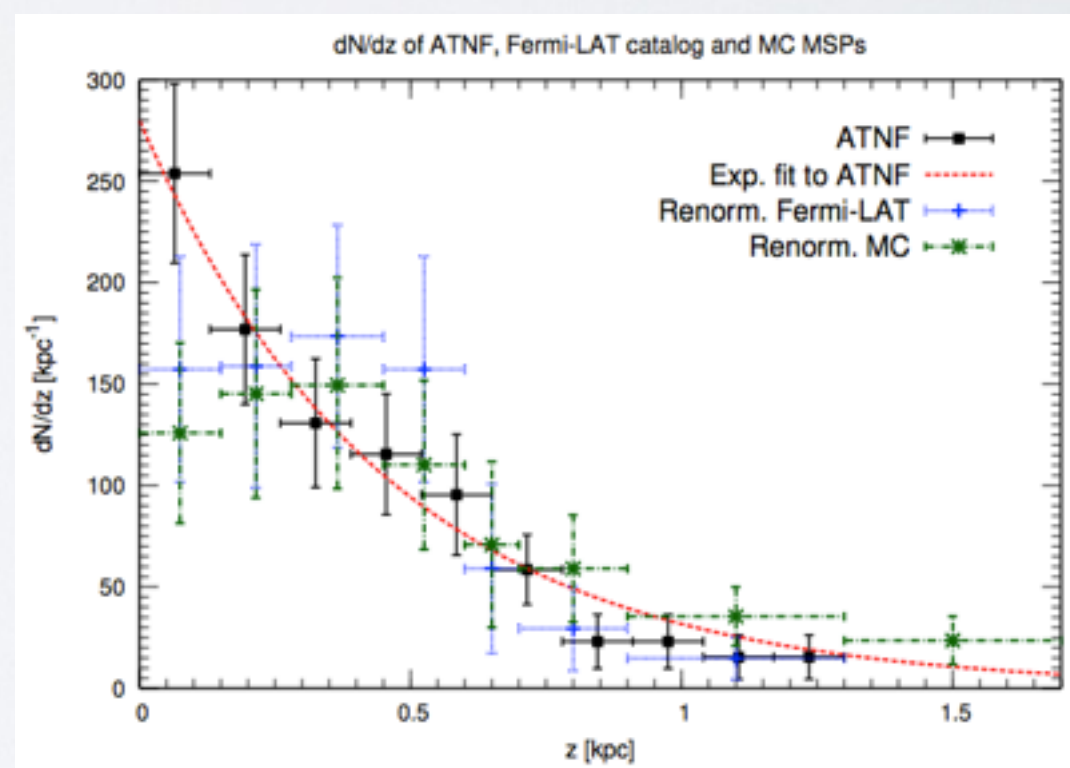

ACTIVE GALACTIC NUCLEI (AGN)

Radio quiet (75-80%)

- Seyfert type 1 and 2
- Radio quiet Quasar (QSO)
- Narrow-emission-line X-ray galaxies (NELG)

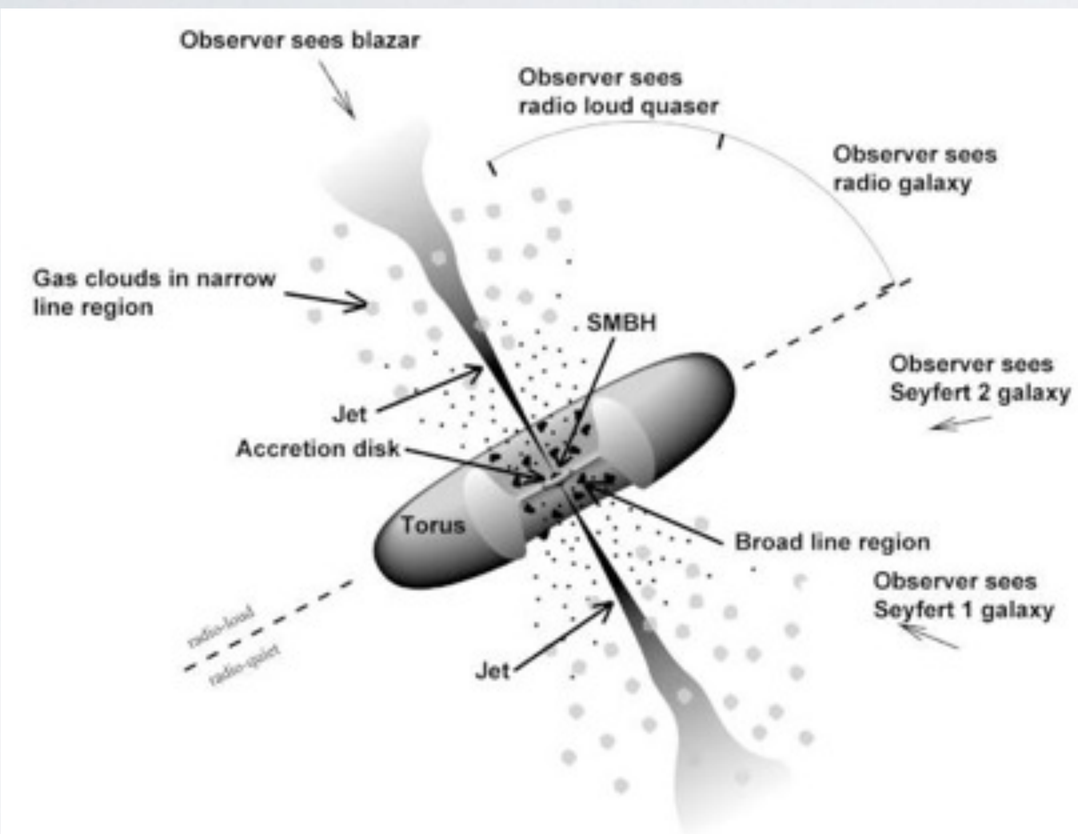

http://www.astro-photography.net/Supermassive-Black-Holes-Active-Galactic-Nuclei.html

Urry and Padovani 1995PASP 107 803U

Radio loud (15-20%)

MISALIGNED (MAGN) φ>14°

BLAZARS φ<14°

- Steep Spectrum Radio Quasars (SSRQ) 14°<φ<40°
- Radio Galaxies (RG) φ>40°

- **BL Lac**: low L_r, brighter in the center and no emission lines

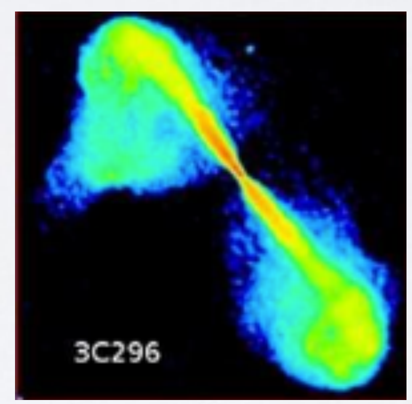

- **FR I** RG: low L_r, brighter in the center and no emission lines

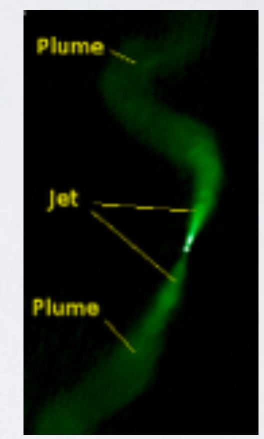

- **FSRQ** high $L_{r,}$ bighter in the lobe with hot spots and with emission lines.

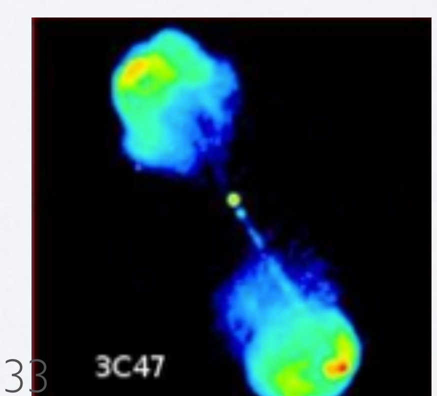

- **FR II** RG high $L_{r,}$ bighter in the lobe with hot spots and with emission lines.

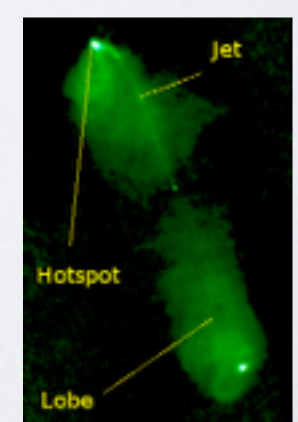

CASCADE COMPONENT

The cascade emission, where $t_{IC}(z)$ is the energy-loss time of an electron, is:

$$\frac{dF_\gamma^{casc}}{d\epsilon}(\epsilon, z) = \frac{(1+z)}{4\pi d_L(z)^2}\int_{\gamma_{e,min}}^{\gamma_{e,max}} \frac{dN_{\gamma_e \epsilon}}{dtd\epsilon}\frac{dN_e}{d\gamma_e} t_{IC}(z) d\gamma_e$$

$$\frac{dN_{\gamma_e \epsilon}}{dtd\epsilon} = \frac{3\sigma_T c}{4\gamma_e^2}\int_0^1 \frac{dx}{x}\frac{dn_{CMB}}{dx}(x(\xi, \gamma_e), z) f(x)$$

Electron spectrum.

$$\frac{dN_e}{d\gamma_e} = \frac{d_L(z)^2}{(1+z)}\frac{d\epsilon_{\gamma,i}}{d\gamma_e}\frac{dF_\gamma}{d\epsilon}\left(1 - \exp\left(-\tau_{\gamma,\gamma}\right)\right)$$

IC scattered photon spectrum per unit time

Intrinsic photon flux

$$\frac{dF_\gamma}{d\epsilon} = \frac{(1+z)^{2-\Gamma}}{4\pi d_L(z)^2}\frac{(2-\Gamma)}{\left[\left(\frac{\epsilon_2}{\epsilon_1}\right)^{2-\Gamma} - 1\right]}\left(\frac{\epsilon}{\epsilon_1}\right)^{-\Gamma}\frac{L_\gamma}{\epsilon_1^2}$$

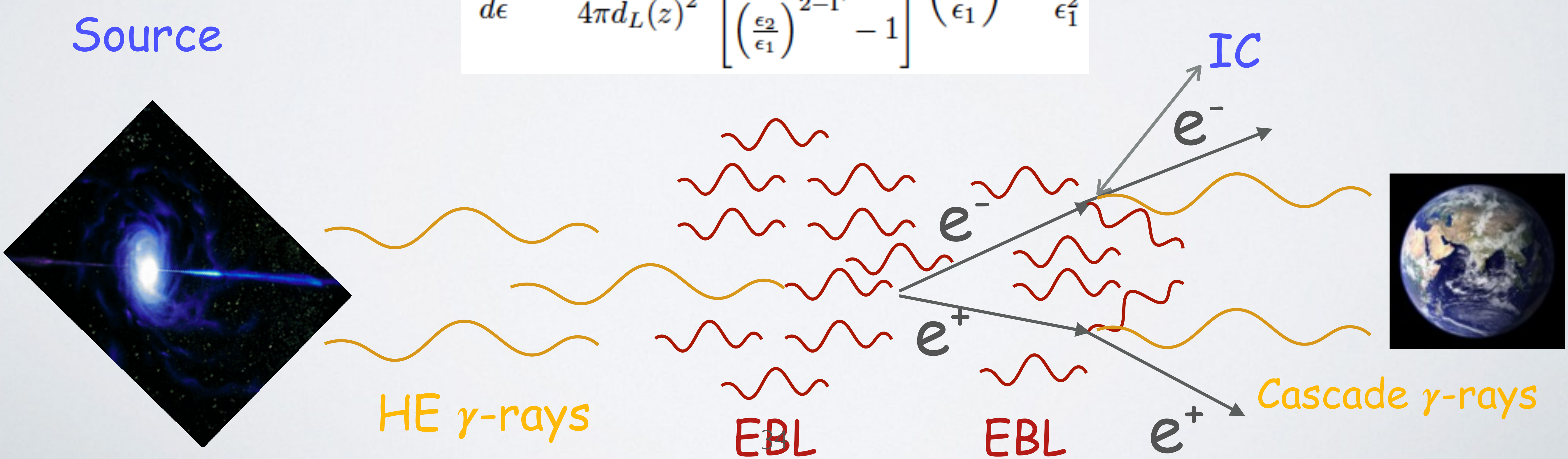

EBL MODELS

Fermi Coll.

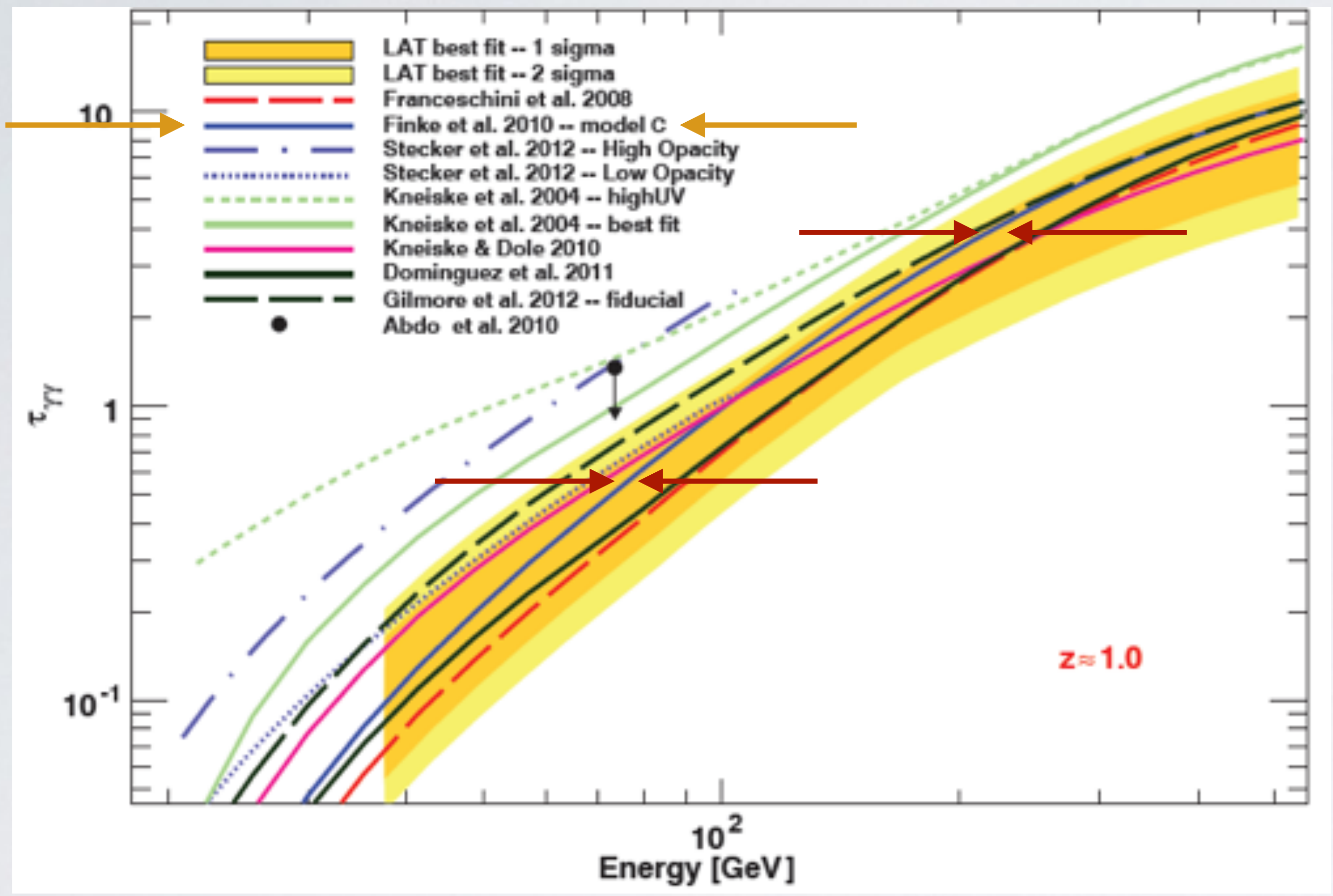

Hess Coll.

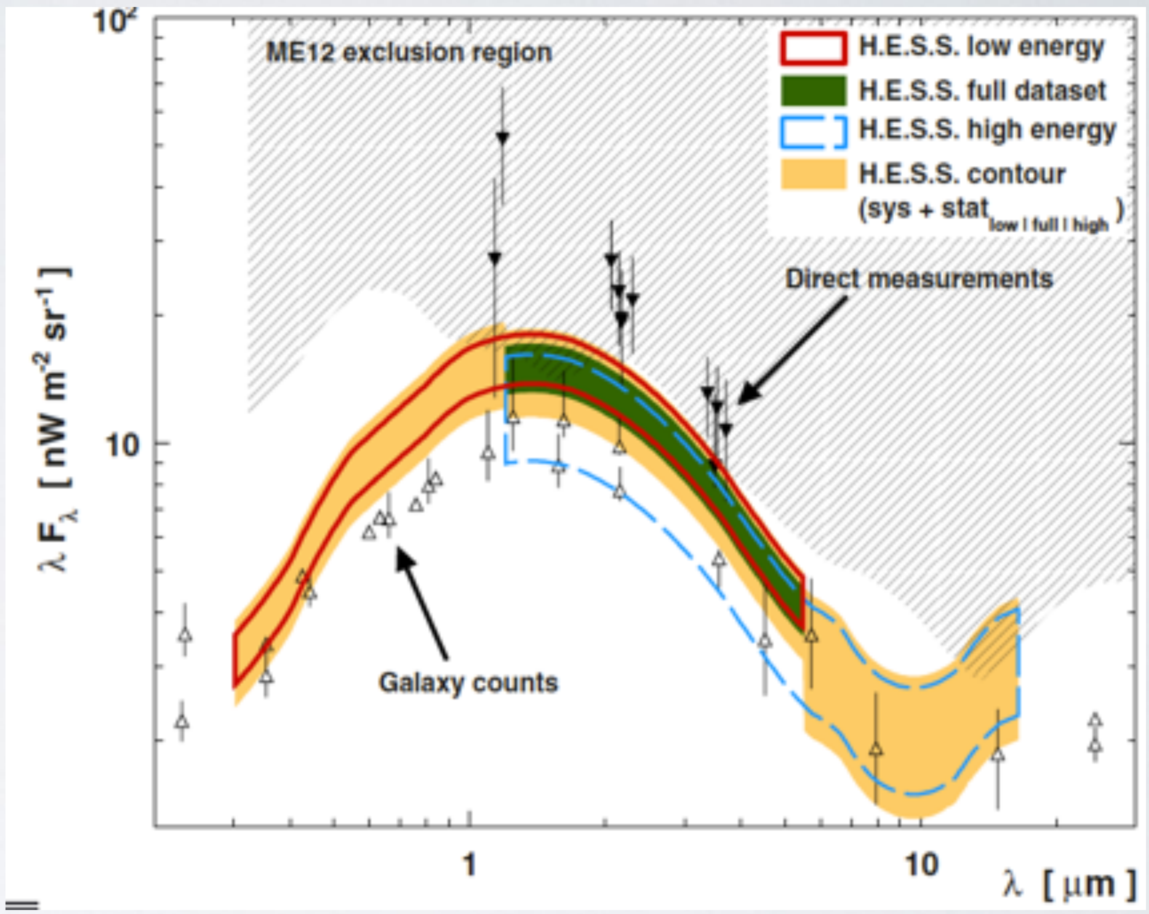

- Constraints on EBL have been derived by Fermi-LAT and HESS Collaboration considering the spectra of brightest blazars.
- All "modern" models from Franceschini et al. 2008 onward survive.
- The next generation of instruments will set more stringent constraints on the nature of EBL.

BLLAC EXPECTED CONTRIBUTION TO IGRB

- Fermi-LAT collaboration is going to publish new data on the IGRB up to 800 GeV.
- High energy data are not explained by the current study of MAGN, Pulsars, SFG and FSRQ.
- The sources population could contribute in a so high energy range should be near (low redshift) and with an hard spectra.
- BL LAC AGNs could be the perfect candidates to contribute with a sizable flux at these high energy.
- These new data are useful also to constraint the indirect dark matter search.

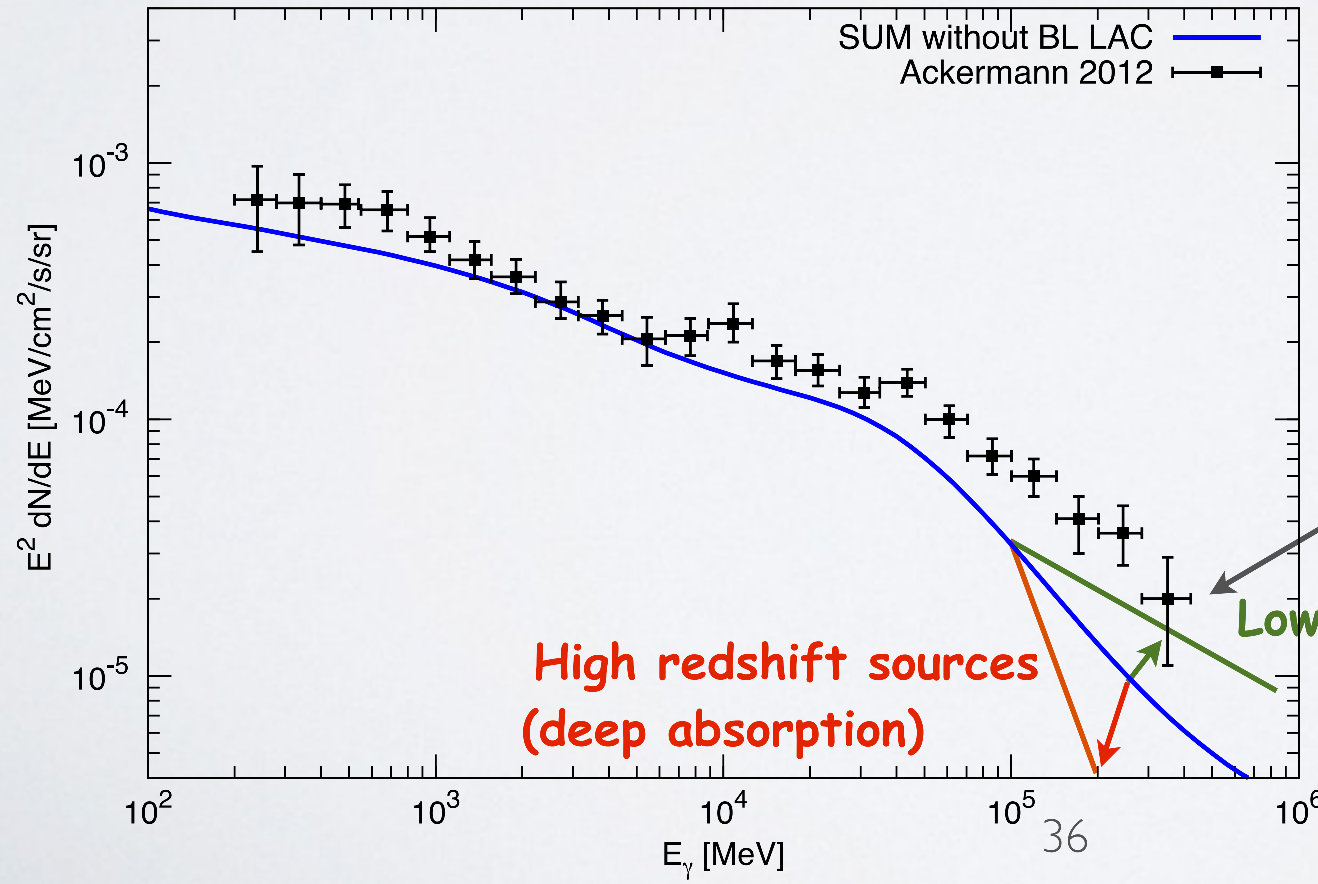

FSRQ CONTRIBUTION

- The first LAT AGN catalog associates 483 of the high-latitude 1FGL sources (|b| > 15°) and TS>50 with AGNs of various types. 186 of which are classified as FSRQs. The faintest identified FSRQ has a 100 MeV–100 GeV band flux of $F \approx 10^{-8}$ photons cm^{-2} s^{-1}.
- Ajello et al. 2012 (ApJ 751:108 2012) used this sample of 186 sources to calculate the unresolved diffuse gamma-ray emission from FSRQ.

FSRQs are LSPs and their SED peak at 10-1000 MeV. For E>100 GeV the SED is negligible.

The flux from unresolved FSRQ follow the same trend of the SED.
FSRQ contribute to IGRB for a 9% to IGRB

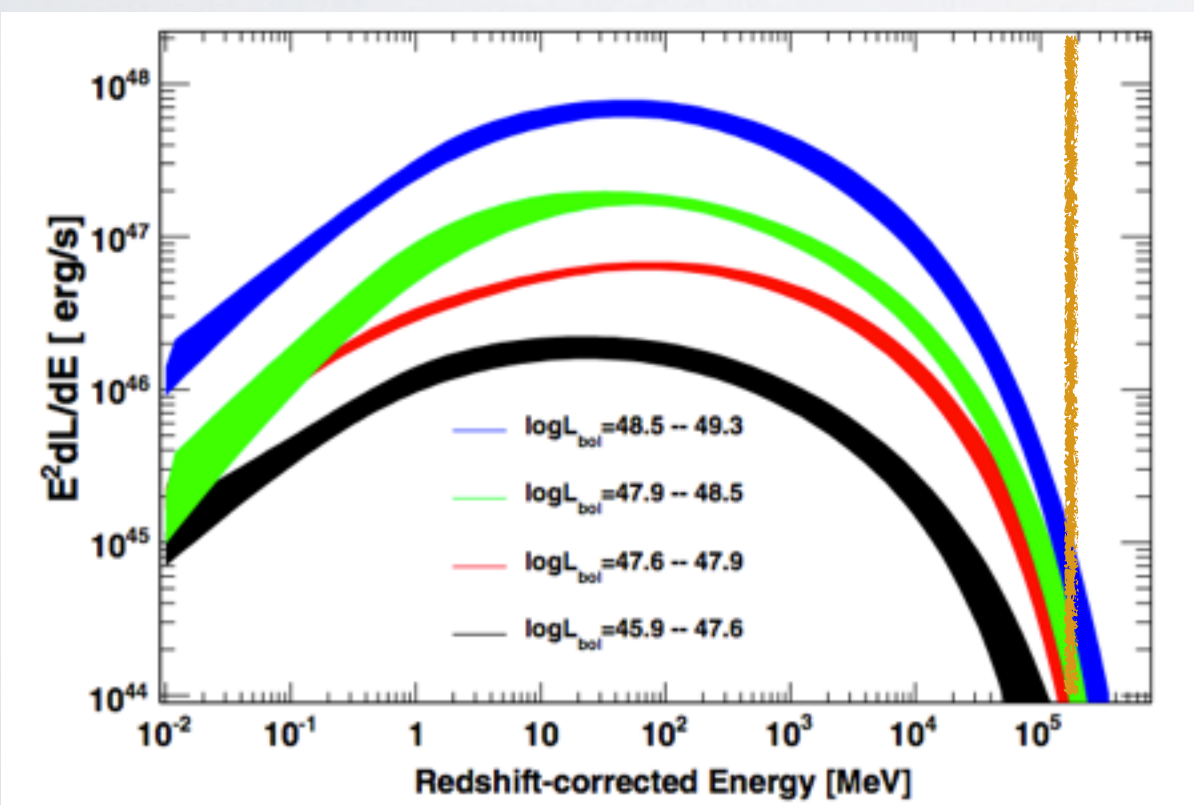

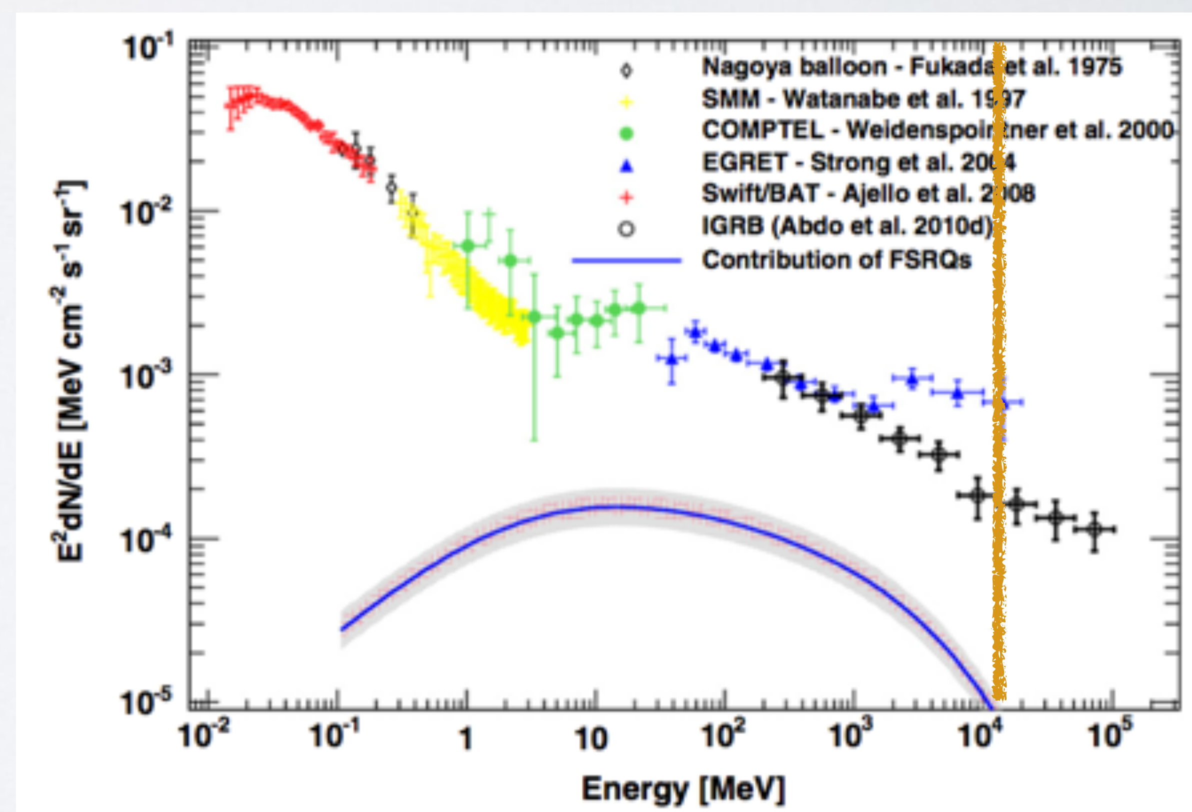

Ajello et al. 2012 (ApJ 751:108 2012)

BL LACERTAE AND FSRQ

Ackermann et al. 2011 ApJ 743:171 011

- There is a relation between the position of the synchrotron peak and the photon spectral index.
- FSRQ which have the lowest values of the synchrotron peak and are the softest Blazars.
- HSP BL Lac are the Blazars with the highest values of the synchrotron peak and which are the soft hardest Blazars.

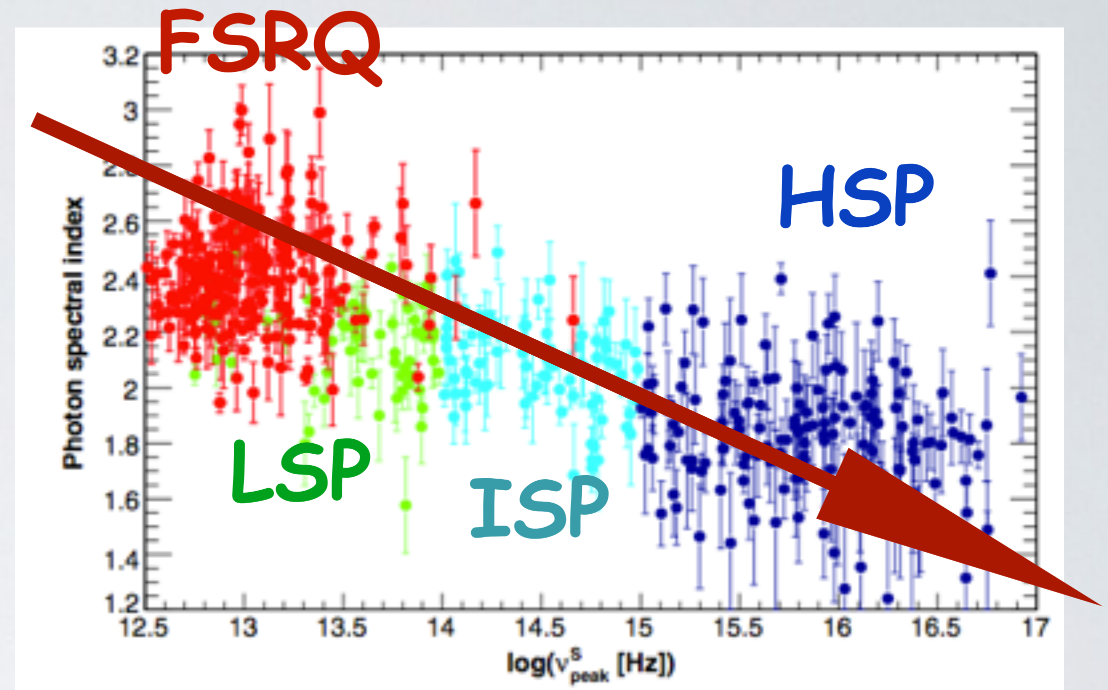

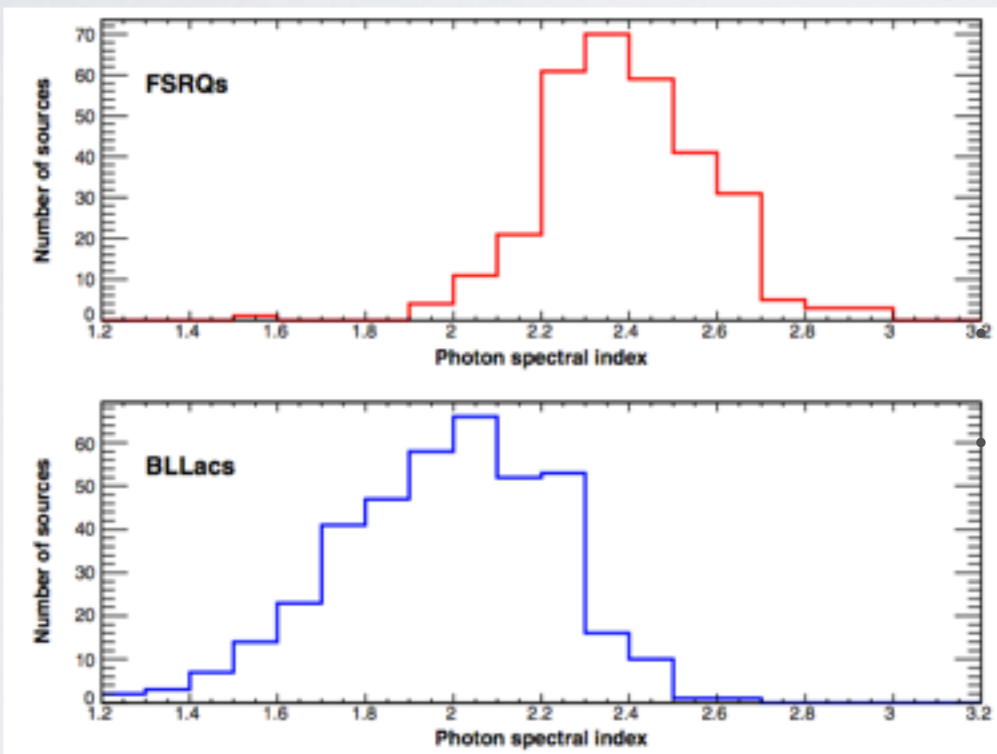

BL Lacs medium photon index Γ = 2.09±0.19

FSRQ have hard spectra Γ = 2.45± 0.20

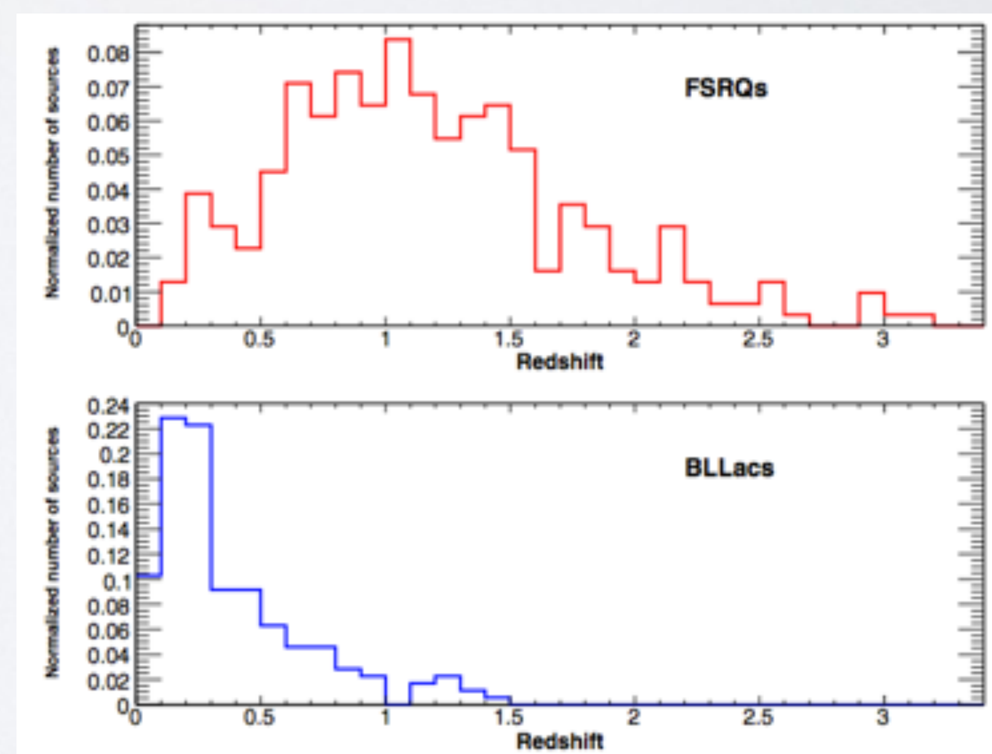

- BL Lac: The redshift distribution peaks around z = 0.2 and extends to z = 1.5.
- FSRQ: The redshift distribution peaks around z = 1 and extends to z = 3.10.

Ackermann et al. 2011 ApJ 743:171 011

FERMI-LAT BLLAC

PHOTON INDEX DISTRIBUTION

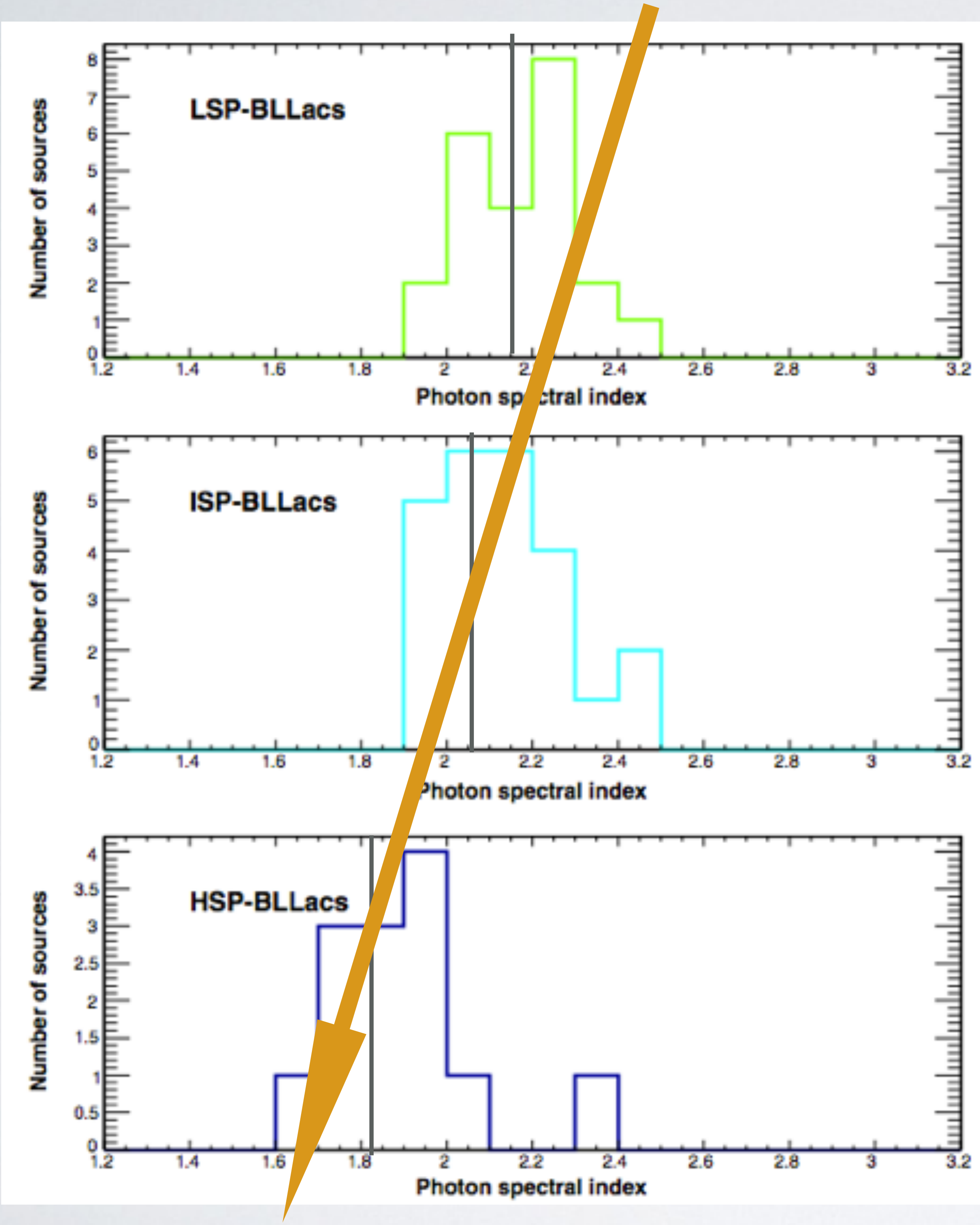

REDSHIFT DISTRIBUTION

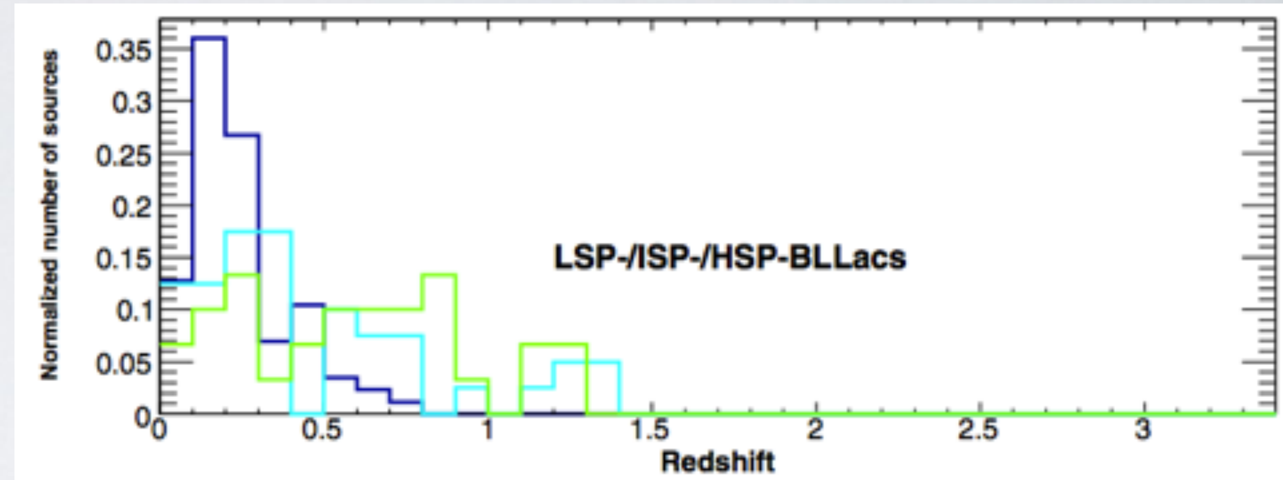

- In the 2FGL 423 BL Lac. 302 (76% of the total) have an SED classification.
- HSPs 53% of SED-classified sources, ISPs the second largest (27%), and LSPs the smallest subclass (20%).
- The BL LAC redshift distribution peaks at a lower redshift.
- 56% of the BL Lac objects have no measured redshifts. The fraction of BL Lac objects having a measured redshift is higher for sources with an SED- based classification. This fraction is essentially constant for the different subclasses.

BL LAC POPULATION

- BL LAC blazars are divided into LSP, ISP and HSP respect to the position of the synchrotron peak.
- BL LAC diffuse γ-ray emission could be found considering separately LSP, ISP and HBL with a spectra of a power-law and an exponential cut off.

SED best fit parameters

	PWL		LP			PLEC		
	Γ_{pow}	$\tilde{\chi}^2$ (d.o.f.)	α	β	$\tilde{\chi}^2$ (d.o.f.)	Γ_{cut}	E_{cut} [GeV]	$\tilde{\chi}^2$ (d.o.f.)
LSP	2.18 ± 0.12	3.4 (114)	2.13 ± 0.13	-1.05 ± 0.30	1.25 (113)	2.08 ± 0.13	34^{+85}_{-20}	0.80 (113)
ISP	2.15 ± 0.14	2.6 (130)	2.12 ± 0.14	-1.08 ± 0.33	1.10 (129)	2.07 ± 0.14	39^{+80}_{-20}	0.49 (129)
LISP	2.17 ± 0.15	3.0 (246)	2.13 ± 0.15	-1.06 ± 0.33	1.15 (245)	2.08 ± 0.15	37^{+85}_{-20}	0.63 (245)
HSP	1.89 ± 0.15	5.4 (248)	1.87 ± 0.14	-1.25 ± 0.26	1.34 (247)	1.86 ± 0.16	910^{+1100}_{-450}	0.48 (247)

PLEC BEST FIT

- LSP: Γ = 2.08±0.13 and Ecut =34^{+85}_{-20} GeV
- ISP: Γ = 2.07±0.14 and Ecut =40^{+80}_{-20} GeV

→ **LISP: Γ = 2.05±0.16 and Ecut =36^{+100}_{-30} GeV**

- **HSP: Γ = 1.86±0.16 and Ecut = 910^{+1100}_{-450} GeV**

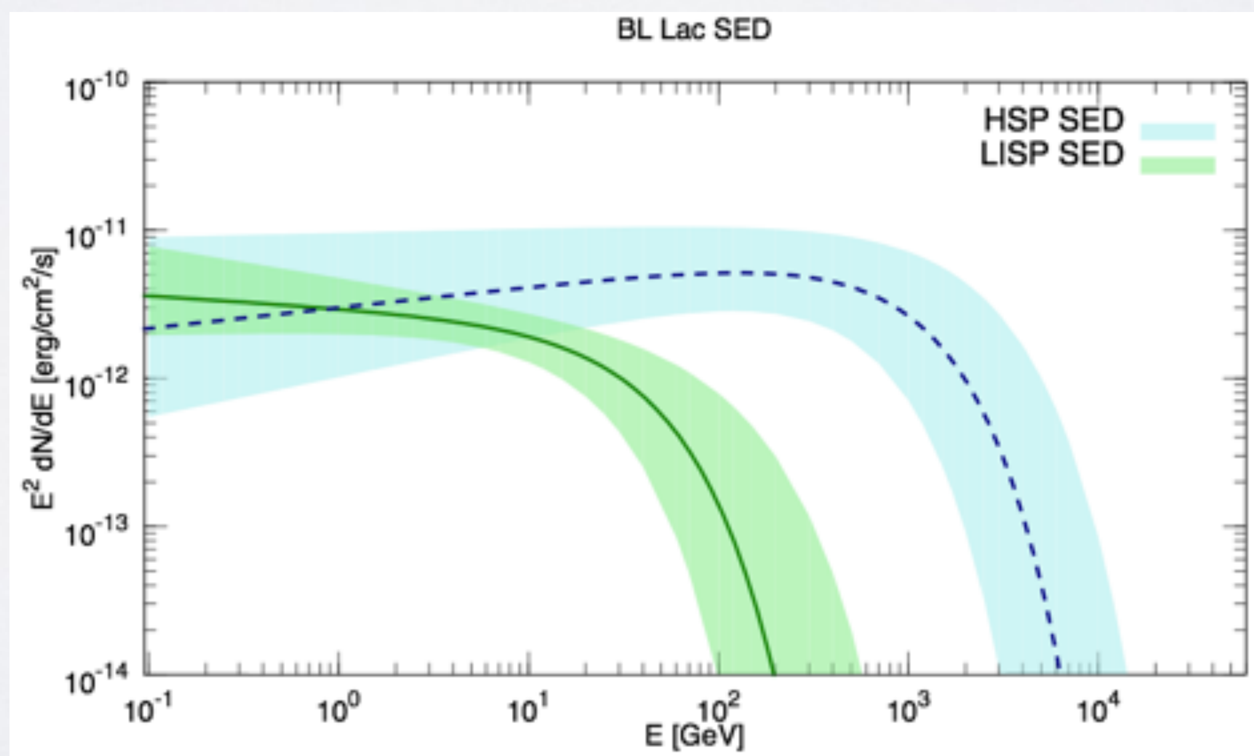

γ-RAY LUMINOSITY FUNCTION SAMPLE

- We have considered the 2FGL catalog.
- Taken into account all the BL Lac with a measured redshift, a SED classification.
- The sample is composed by 80 HSP, 34 ISP and 34 LSP.
- The incompleteness of the sample is: (80 + 11 + 102 + 37)/80 ≈ 2.88 for HSP and (34 + 5 + 43 + 16)/34 ≈ 2.88 for LSP and ISP.
- We have taken into account the incompleteness of the sample correcting upward the normalization of the LF as to reflect the inferred actual number of BL Lacs.

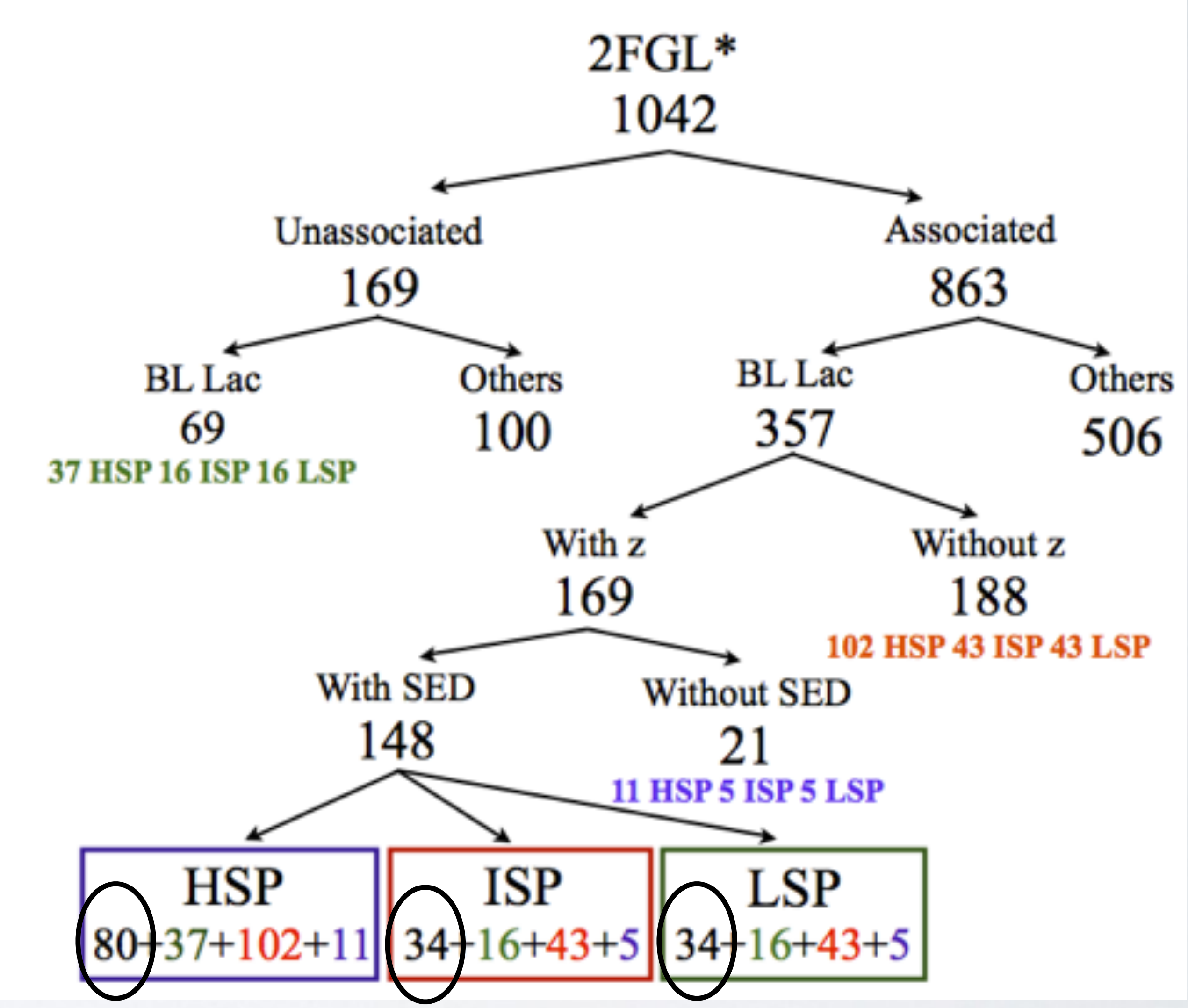

γ-RAY LUMINOSITY FUNCTION

- The space density of BL Lac is defined by:

$$\Theta_\gamma(z,\Gamma,L_\gamma) = \frac{d^3N}{dz\,d\Gamma\,dL_\gamma} = \frac{d^2N}{dV\,dL_\gamma}\frac{dV}{dz}\frac{dN}{d\Gamma} = \rho_\gamma(z,L_\gamma)\frac{dV}{dz}\frac{dN}{d\Gamma}$$

- where: $\rho(z,L_\gamma) = \frac{d^2N}{dV\,dL_\gamma}$ is the γ-ray luminosity function and $\frac{dN}{d\Gamma} = e^{\frac{(\Gamma-\mu)^2}{2\sigma^2}}$ is the photon index distribution.

- In order to find ρ we take into account three theoretical functions: the **Pure Luminosity Evolution** (PLE, Hasinger et al. 2005; Ueda et al. 2003), the **Luminosity-dependent Density Evolution** (LDDE, Ueda et al. 2003) and the **Steep-Spectrum Radio Sources** (SSRS, Willott et al. 2001) models.

- For each model we find the values of the parameters in order to fit the data.

Experimental

$$\frac{dN}{dz} = \frac{1}{\Delta z}\sum_{i=1}^{N_z}\frac{1}{\Delta\Omega},$$

$$\frac{dN}{dL_\gamma} = \frac{1}{\Delta L_\gamma}\sum_{i=1}^{N_{L_\gamma}}\frac{1}{\Delta\Omega},$$

$$N(>F_\gamma) = \sum_{i=1}^{N(>F_{\gamma,i})}\frac{1}{\Delta\Omega\,\omega(F_{\gamma,i})},$$

Theoretical

$$\frac{dN}{dz} = \int_{\Gamma_{\min}}^{\Gamma_{\max}} d\Gamma \int_{L_\gamma^{\min}}^{L_\gamma^{\max}} dL_\gamma\,\Theta_\gamma(z,\Gamma,L_\gamma)\,\omega(F_\gamma),$$

$$\frac{dN}{dL_\gamma} = \int_{\Gamma_{\min}}^{\Gamma_{\max}} d\Gamma \int_{z_{\min}}^{z_{\max}} dz\,\Theta_\gamma(z,\Gamma,L_\gamma)\,\omega(F_\gamma),$$

$$N(>F_\gamma) = \int_{\Gamma_{\min}}^{\Gamma_{\max}} d\Gamma \int_{z_{\min}}^{z_{\max}} dz \int_{L_\gamma(F_\gamma,z,\Gamma)}^{L_\gamma^{\max}} dL_\gamma\,\Theta_\gamma(z,\Gamma,L_\gamma),$$

BL LAC DISTRIBUTIONS

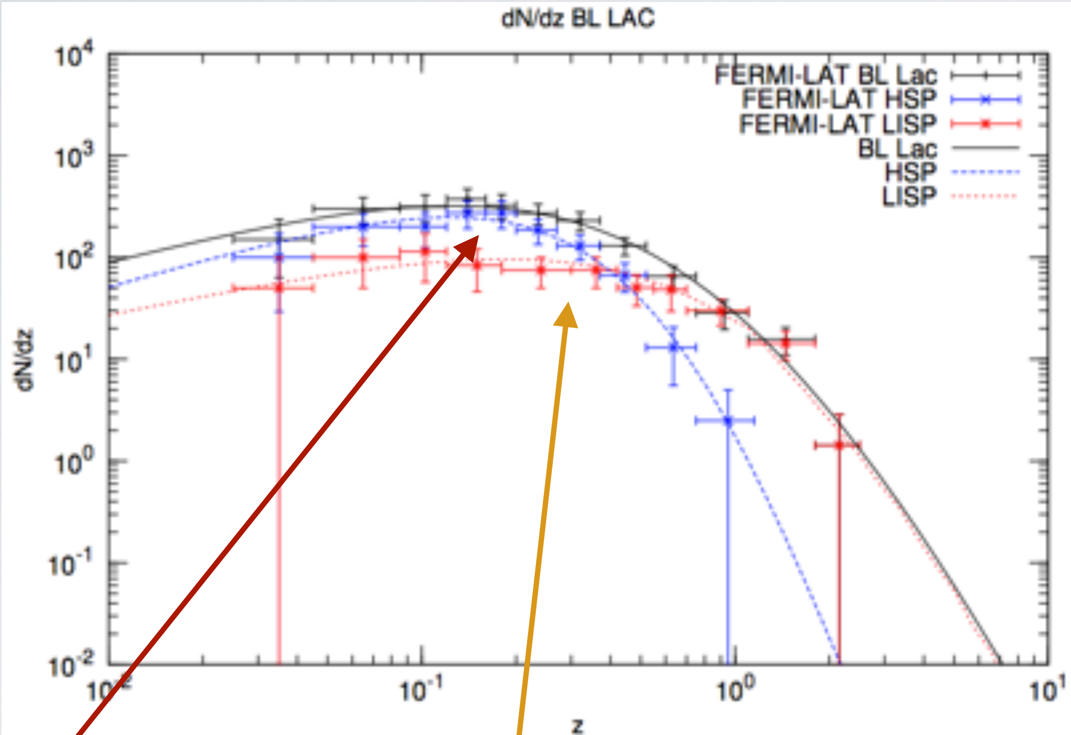

HSPs have a narrow redshift distribution peaked around 0.2, while the LISPs have a broader distribution which extends to z ≈ 2.

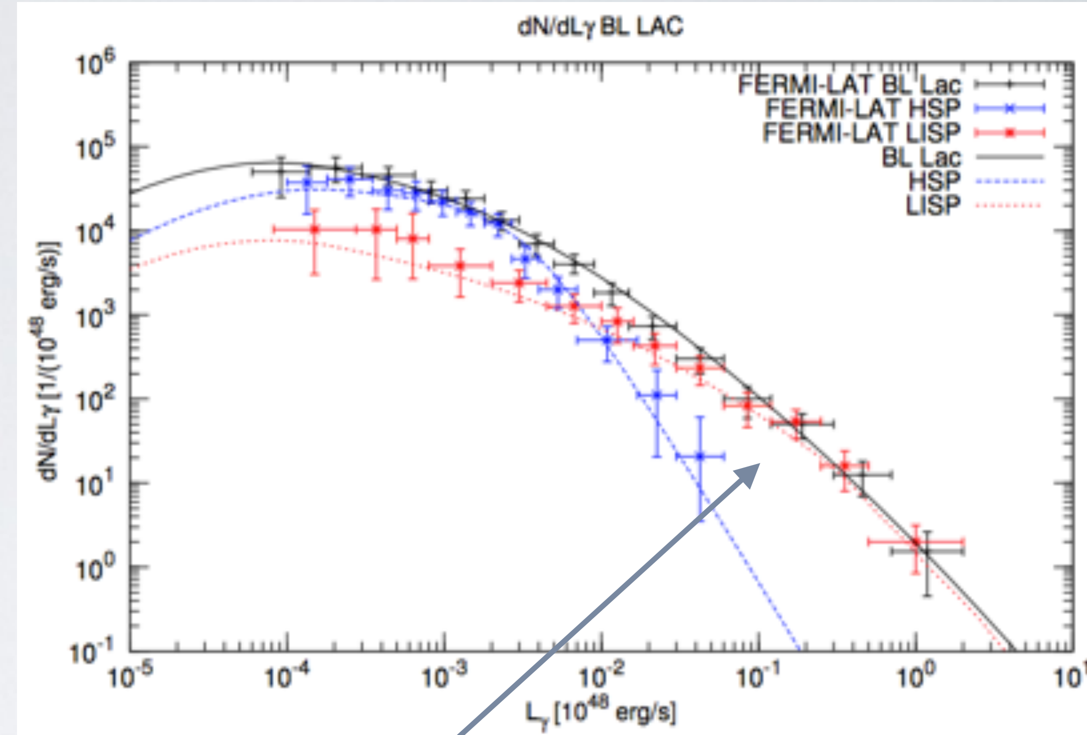

LSPs are more luminous than HSPS

LDDE the best model to represent the luminosity function.

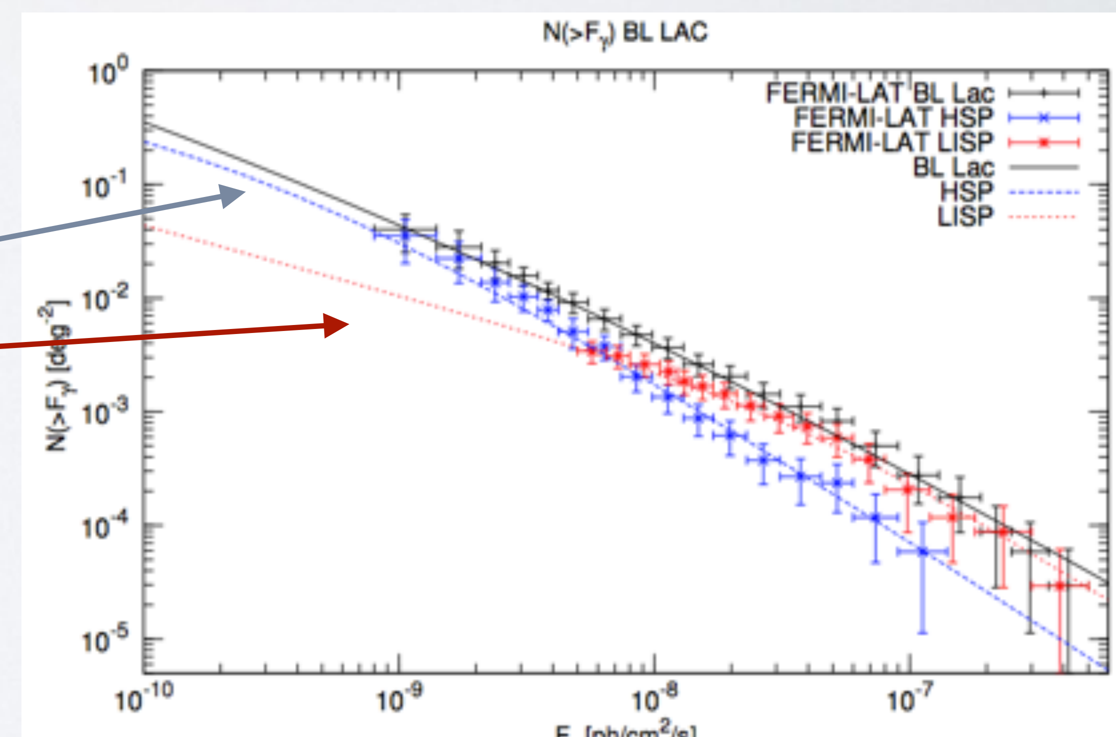

The source count distribution shows that there are more high-flux LISPs than HSPs, while the opposite trend is present for low values of Fγ.

We expect therefore the bulk of the flux to be due to HSPs, which are much more numerous than LISPs for very low Fγ

2FGL EFFICIENCY

- We have considered the 2FGL catalogue so we should use the second catalogue efficiency which has not been calculated by the collaboration.

- We found so an empirical efficiency for the 2FGL catalogue for TS>25 and |b|>10° using the following method.

Number of blazars in the 2FGL catalogue with TS>25 and |b|>10° and with a flux comprised in the bin i.

$$\omega(F_\gamma^i) = (1+\eta)\frac{N_{blazars}(F_\gamma^i)}{\Delta\Omega \int_{F_\gamma^{i,min}}^{F_\gamma^{i,max}} \frac{dN}{dF_\gamma} dF_\gamma}$$

Number of expected sources calculated using the flux distribution of blazars of the 1FGL

(Abdo et al. 2010 ApJ 720:435–453)

Incompleteness of the 2FGL: ratio between the number of unidentified sources and all the sources with TS>25 and |b|>10°

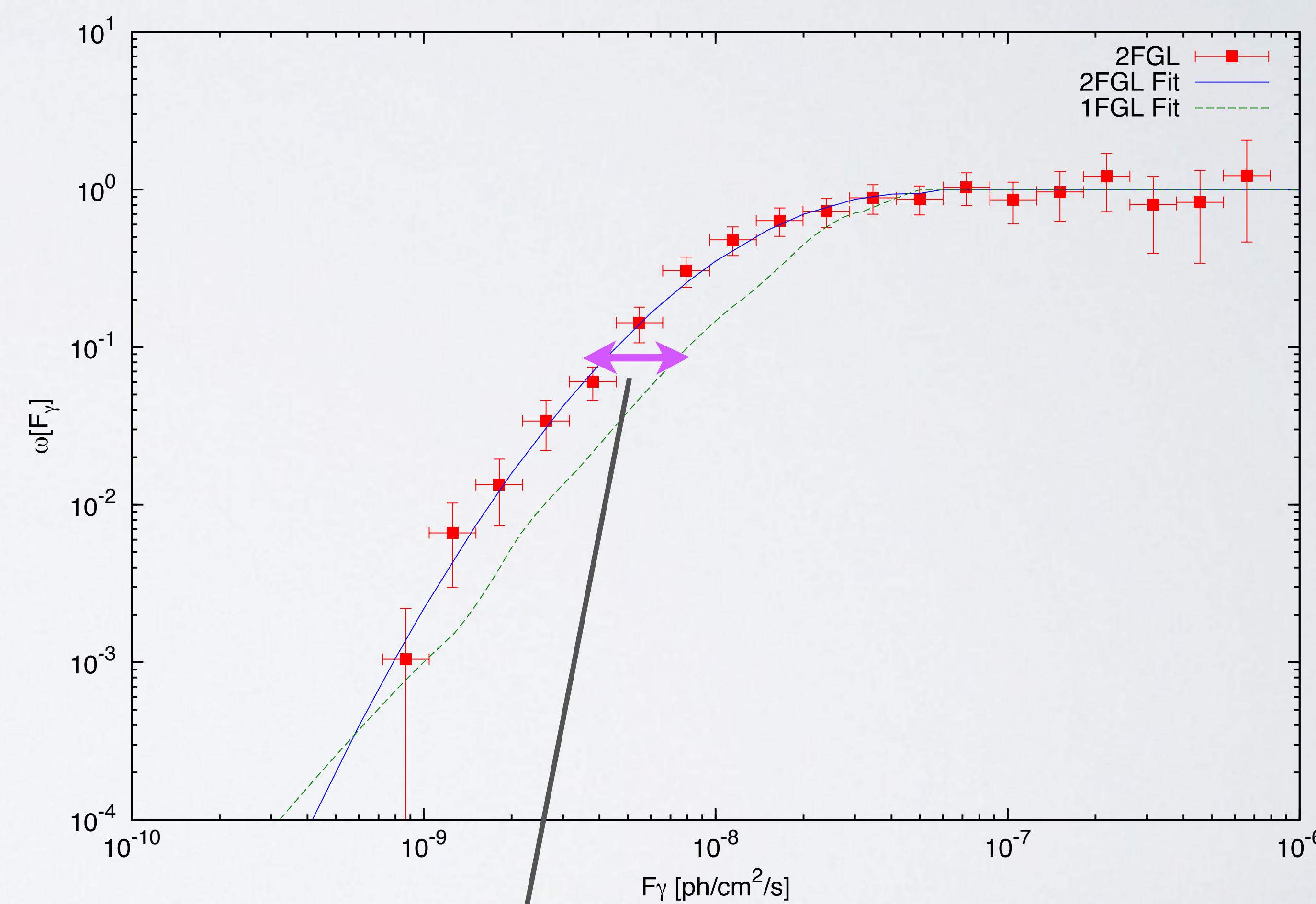

1FGL EFFICIENCY TS>50 and |b|>20°

2FGL EFFICIENCY TS>25 and |b|>10°

BURKERT PROFILE

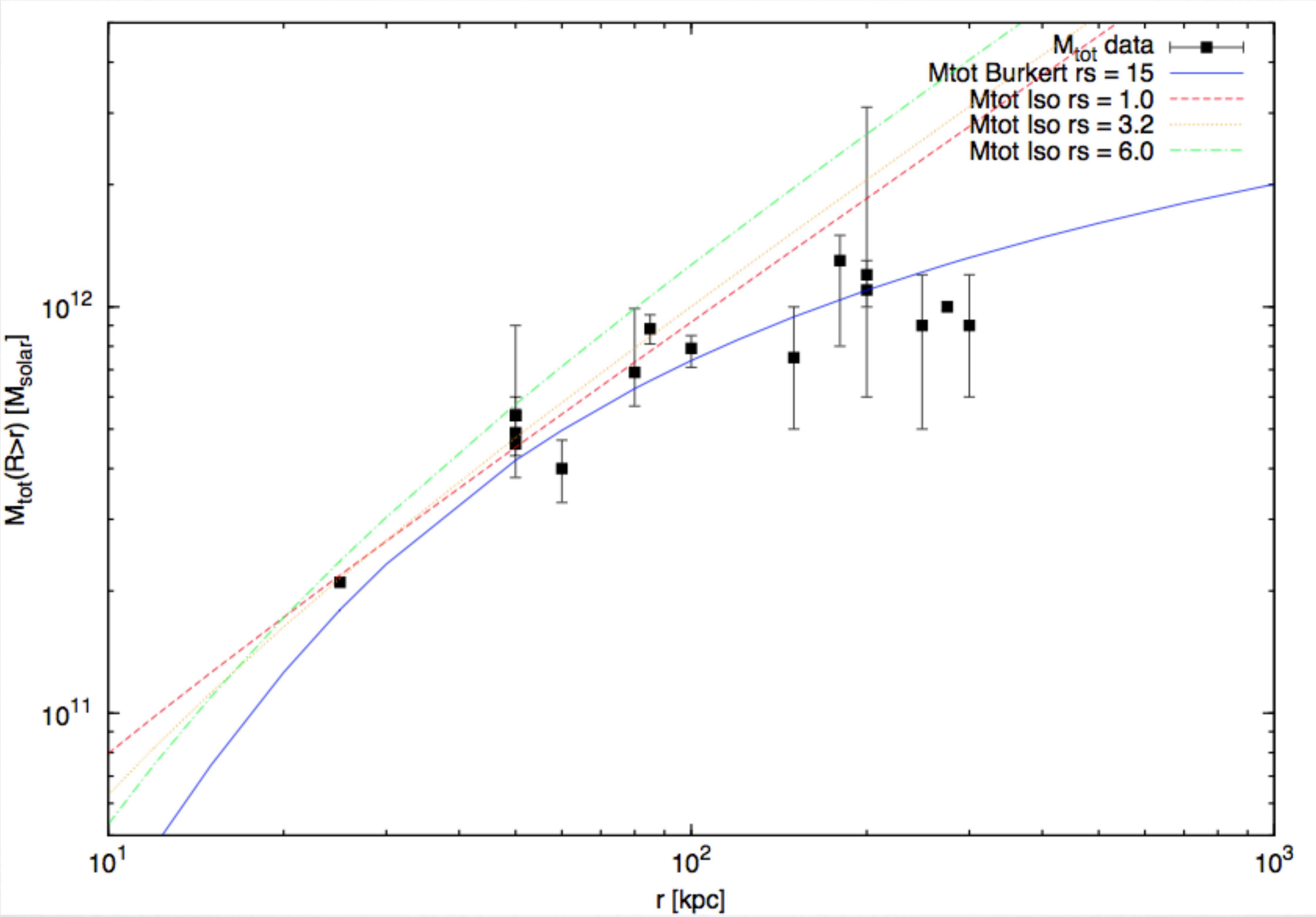

POPULATIONS

- An **active galactic nucleus (AGN)** is a compact region at the centre of a galaxy that has a much higher than normal luminosity over at least some portion, and possibly all, of the electromagnetic spectrum. Such excess emission has been observed in the radio, infrared, optical, ultra-violet, X-ray and gamma ray wavebands. A galaxy hosting an AGN is called an active galaxy. The radiation from AGN is believed to be a result of accretion of mass by a supermassive black hole at the centre of its host galaxy.
- **Blazars** are considered as radio-loud AGN with the relativistic jet pointing in the direction of the observer (Urry & Padovani 1995). Their spectral energy distribution (SED) is thus dominated by the non-thermal emission from the jet, enhanced by relativistic effects.
- The **blazars** class is divided into the two subclasses according to the strength of the non-thermal continuum emission relative to the thermal emission from the accretion disc that is partially reprocessed in the broad-line-region (BLR).
- **Flat-spectrum-radio-quasars (FSRQs)** if emission lines and/or the big blue bump are observed.
- **BL Lacertae (BL Lac)** objects if the optical/UV spectrum is dominated by the continuum emission
- **Star forming galaxies**: structure formation in the intergalactic medium (IGM) produces large-scale, collisionless shock waves, in which electrons can be accelerated to highly relativistic energies. Such electrons can Compton-scatter cosmic microwave background photons up to γ-ray energies. We study the radiation

  emitted in this process using a hydrodynamic cosmological simulation of a CDM universe. The resulting radiation, extending beyond TeV energies, has roughly constant energy flux per decade in photon energy, in agreement with the predictions of Loeb & Waxman